



Air pollution in heavy industrial cities along the northern slope of the Tianshan Mountains, Xinjiang: characteristics, meteorological influence, and sources

Yutian Luo¹ · Liping Xu¹ · Zhongqin Li^{1,2,3} · Xi Zhou⁴ · Xin Zhang² · Fanglong Wang² · Jiajia Peng¹ · Cui Cao¹ · Zhi Chen¹ · Heng Yu³

Received: 11 November 2022 / Accepted: 1 February 2023 / Published online: 8 March 2023
© The Author(s), under exclusive licence to Springer-Verlag GmbH Germany, part of Springer Nature 2023

Abstract

The spatiotemporal characteristics, relationship with meteorological factors, and source distribution of air pollutants (January 2017–December 2021) were analyzed to better understand the air pollutants on the northern slope of the Tianshan Mountains (NSTM) in Xinjiang, a heavily polluted urban agglomeration of heavy industries. The results showed that the annual mean concentrations of SO₂, NO₂, CO, O₃, PM_{2.5}, and PM₁₀ were 8.61–13.76 μg m⁻³, 26.53–36.06 μg m⁻³, 0.79–1.31 mg m⁻³, 82.24–87.62 μg m⁻³, 37.98–51.10 μg m⁻³, and 84.15–97.47 μg m⁻³. The concentrations of air pollutants (except O₃) showed a decreasing trend. The highest concentrations were in winter, and in Wujiaqu, Shihezi, Changji, Urumqi, and Turpan, the concentrations of particulate matter exceeded the NAAQS Grade II during winter. The west wind and the spread of local pollutants both substantially impacted the high concentrations. According to the analysis of the backward trajectory in winter, the air masses were mainly from eastern Kazakhstan and local emission sources, and PM₁₀ in the airflow had a more significant impact on Turpan; the rest of the cities were more affected by PM_{2.5}. Potential sources included Urumqi–Changji–Shihezi, Turpan, the northern Bayingol Mongolian Autonomous Prefecture, and eastern Kazakhstan. Consequently, the emphasis on improving air quality should be on reducing local emissions, strengthening regional cooperation, and researching trans-boundary transport of air pollutants.

Keywords Air pollutants · Spatio-temporal variations · Meteorological conditions · Potential source · Northern slope of the Tianshan Mountains (NSTM)

Responsible Editor: Gerhard Lammel

✉ Liping Xu
xlp_tea@shzu.edu.cn

Xi Zhou
zhouxi13_lzu@163.com

¹ College of Sciences, Shihezi University, Xinjiang 832003, China

² State Key Laboratory of Cryospheric Sciences, Northwest Institute of Eco-Environment and Resources, Tianshan Glaciological Station, Chinese Academy of Sciences, Lanzhou 730000, China

³ College of Geography and Environmental Science, Northwest Normal University, Lanzhou 730070, China

⁴ Key Laboratory of Western China's Environmental Systems (Ministry of Education), College of Earth and Environmental Sciences, Lanzhou University, Lanzhou 730000, China

Introduction

Significant air pollution challenges have emerged in China due to the country's rapid economic development, industrialization, and urbanization (Geng et al. 2021; Song et al. 2017; Kan et al. 2012). People often live in polluted air, which can lead to poisoning or cancer and is a major risk factor for the disease burden in China (Li and Dai 2022). In particular, the different sources and components of pollutants have a more pronounced impact on health during the cold season (Cao et al. 2009; Chen et al. 2010). According to the *2021 Actions on Quality*, if governments took action to improve air quality, it would prevent 7 million premature deaths each year and help improve the overall health and economic well-being of 92% of the world's population. Air pollution, especially fine particulate pollution, has become a serious environmental problem in China (Hu et al. 2014) and poses a threat to human health (Geng et al. 2019; Zhao et al.

2018a; Li et al. 2018a; Cohen et al. 2017). $PM_{2.5}$ concentrations for all of China's population still exceed the WHO air quality guidelines, and 81.1% of them still live in areas that exceed WHO Interim Target 1 (the least stringent WHO interim air quality objective of $35 \mu\text{g m}^{-3}$), demonstrating that China still faces challenges with ambient particulate matter pollution (Yin et al. 2020). Since 2013, certain large cities' national air quality monitoring stations have started to receive approval from the Ministry of Environmental Protection for the measurement of six criterion air pollutants, including sulfur dioxide (SO_2), nitrogen dioxide (NO_2), carbon monoxide (CO), ozone (O_3), and particulate matter ($PM_{2.5}$ and PM_{10} , with an aerodynamic diameter equal to or < 2.5 and $10 \mu\text{m}$, respectively). These data are a prerequisite for the investigation and resolution of China's air pollution issue, and a variety of issues have been researched using data from these monitoring sites (Fan et al. 2020; Ma et al. 2019; Guo et al. 2019; Zhou et al. 2018). Since the implementation of emission control strategies mainly in industry, residential, and transportation, China has gradually accumulated experience and achieved certain results in air pollution control. Air pollutants (except O_3) concentrations in China have decreased significantly over the past few years, but concentrations of SO_2 , CO, $PM_{2.5}$, and PM_{10} still remain high in northwest China (Liu et al. 2020; Fan et al. 2020). By 2017, $PM_{2.5}$ concentrations over the heavily polluted regions of eastern China showed a noticeable downward trend relative to 2013 (Zhang et al. 2019; Wang et al. 2020a). The concentration of air pollutants is significantly influenced by emissions and meteorological conditions (Jhun et al. 2015; Wang et al. 2018; He et al. 2017). Unfavorable meteorological conditions can increase air pollutants when emissions remain constant, and even play a dominant role in some cases (Zhang et al. 2015, 2018). Moreover, even if local emissions are reduced, regional transport may increase air pollutants at the location of interest (Leibensperger et al. 2011; Wang et al. 2009a). Research on the six air pollutants is urgently required. Intensive academic study has currently concentrated on air pollution issues in regions of China with rapid economic development and high human activities, such as Beijing–Tianjin–Hebei, the Yangtze River Delta, the Pearl River Delta, and the Sichuan Basin (Zhou et al. 2020; Qi et al. 2017; Yuan et al. 2021; Zhao et al. 2018b); however, less attention has been paid to the northern slope of the Tianshan Mountains (NSTM).

The NSTM is the political, economic, and cultural center of the Xinjiang Uygur Autonomous Region (hereinafter Xinjiang), as well as the northwestern agglomeration of the country. In the last decade, the region's annual GDP has exceeded 50% of the GDP of Xinjiang, gathering many industrial enterprises, with a coal-based energy structure, an industrial structure with a large proportion of heavy industry, and a transportation structure with road freight

emitting enormous pollutants (Fang 2019). In the study area, the non-heating period is characterized by a large environmental capacity, favorable diffusion conditions, and positive regional air quality. However, as the heating period approaches, the local environment's capacity for handling pollutants decreases, diffusion conditions deteriorate, and the combination of unfavorable meteorological factors influences, resulting in more frequent heavily polluted weather during the heating period. The NSTM has one of China's highest annual average $PM_{2.5}$ concentrations (Shen et al. 2019). Wang et al. (2020b) explored the spatio-temporal variation characteristics of $PM_{2.5}$ concentrations in this place and concluded that $PM_{2.5}$ concentrations were high and increased significantly from 2001 to 2016. Wang et al. (2014a) observed that the annual mean concentrations of PM_{10} on the NSTM ranged from 55 ± 28 to $92 \pm 75 \mu\text{g m}^{-3}$ (2007–2013), with heavy anthropogenic air pollution in winter. Ma et al. (2022) used near-surface observations obtained from the national air ambient monitoring network in the NSTM region from 2015 to 2019 to examine the variation and drivers of $PM_{2.5}$ and found an exceedance rate of 23.3% ($54.3 \mu\text{g m}^{-3}$) in this region. Although some studies, as described above, have been conducted to investigate pollutants in the NSTM region, they only analyzed one or two pollutants, and there has been a paucity of studies on all six pollutants over a long period of time. Thus, this study examined six pollutant concentrations over a 5-year period to draw more attention and further research to the serious environmental problems in this region.

Using data from air quality monitoring stations (January 2017–December 2021) in the NSTM, this study analyzed the spatial and temporal characteristics of air pollutants (SO_2 , NO_2 , CO, O_3 , $PM_{2.5}$, and PM_{10}). Rupakheti et al. (2021) studied a similar dataset for 16 cities throughout Xinjiang from 2013 to 2019. Additionally, this study investigated the relationship between concentrations of air pollutants and meteorological factors, as well as the source distribution. In order to comprehend the origins of particulate matter in the study area, backward trajectory, PSCF (potential source contribution function), and CWT (concentration weighted trajectory) analyses were carried out based on HYSPLIT (Hybrid Single-Particle Lagrangian Integrated Trajectory) model in heavily polluted weather. Meteorological conditions are one of the most critical factors affecting air quality (Kang et al. 2019; Tian et al. 2019). Understanding the transport of air pollutants and the impact of potential source areas on the local environment is also essential. Therefore, a more comprehensive air quality study of multiple pollutants on the NSTM is necessary to better understand the air pollution situation in the region. These findings will serve as a prerequisite and the foundation for the scientific development of prevention and control strategies for air pollution.

Data and methods

Study area

The NSTM is the most developed region in Xinjiang in terms of economy, education, science, and technology, as well as an essential hub of the Silk Road Economic Belt to Central Asia and Europe (Development and Reform Commission of Xinjiang Uygur Autonomous Region 2017). The region is distributed in the arid and semi-arid climate zone, a typical temperate continental climate with scarce precipitation, intense evaporation, dusty weather, and large annual and daily temperature differences (Liu et al. 2018). The Taklamakan Desert, China's largest desert, and the Gurbantunggut Desert, China's second-largest desert, respectively, border the northern and southern slopes of the Tianshan Mountains, together with rapid urbanization in recent years, has led to serious urban and regional air pollution problems (Han 2018). Ten cities in the study area, from Hami in the east to Ili Kazakh in the west, are shown in Fig. 1 along with their locations and elevations. Table S1 provides more details on these cities, including longitude, latitude, elevation, population, GDP, and car parc.

Data source and quality control

The concentrations of six criteria pollutants (SO_2 , NO_2 , CO , O_3 , $\text{PM}_{2.5}$, and PM_{10}) and the AQI (Air Quality Index) from 36 monitoring stations in ten cities in the NSTM from 2017 to 2021 used in this study were provided by the China National Environmental Monitoring Center. Daily temperature, relative humidity, wind speed, and wind direction were among the meteorological data that were collected from the China Meteorological Data Service Centre. Downloaded from NOAA (National Oceanic and Atmospheric Administration), the GDAS (Global Data Assimilation System) dataset was used on a global scale in the HYSPLIT model, with a spatial resolution of $1^\circ \times 1^\circ$. Detailed data information is shown in Table S2.

The quality control of the data was validated in accordance with the requirements for the National Ambient Air Quality Standards of China (NAAQS, GB 3095–2012). The values that are missing or ≤ 0 are set to invalid. The calculation of the 24-h average concentrations of each pollutant was only done where there were more than 20 h of valid data available. Eight-hour O_3 concentrations were only estimated when there were at least 6 h of valid data available for every 8 h. Based on less than four invalid days of data every month, the pollutants' monthly average concentrations were computed. When a year had more than 324 days of valid data, annual averages

were declared to be valid. Citywide average concentrations were calculated by averaging the concentrations from all stations in each city. The People's Republic of China's National Environmental Protection Standard (HJ 630–2011) technical standards for environmental monitoring quality management were used to guide the quality assurance and control (QA/QC) of data. This approach has also been employed in a number of previous studies to demonstrate the reliability of the data quality; more details can be seen in Wang et al. (2021) and Fan et al. (2020).

Backward trajectory analysis

Using the HYSPLIT (Hybrid Single-Particle Lagrangian Integrated Trajectory) backward trajectory model in conjunction with the GDAS dataset, 72-h backward trajectories were calculated to identify potential long-range transport paths of air masses approaching cities (Draxler and Rolph 2003). The backward trajectories calculated 500 m above the ground at 00:00, 06:00, 12:00, and 18:00 (UTC) every day were obtained by cluster analysis. A Lagrangian integrated model called HYSPLIT simulates the trajectories of air parcels to determine the paths that air masses travel during transport. In the research of air mass transportation, HYSPLIT is frequently utilized (Yin et al. 2021). Additionally, TrajStat is a Geographic Information System (GIS)-based tool for identifying pollution sources, enabling visualization and statistical analysis of air quality trajectories, and is used extensively in MeteoInfo software as a valuable tool for HYSPLIT simulations (Wang et al. 2009b; Wang 2014).

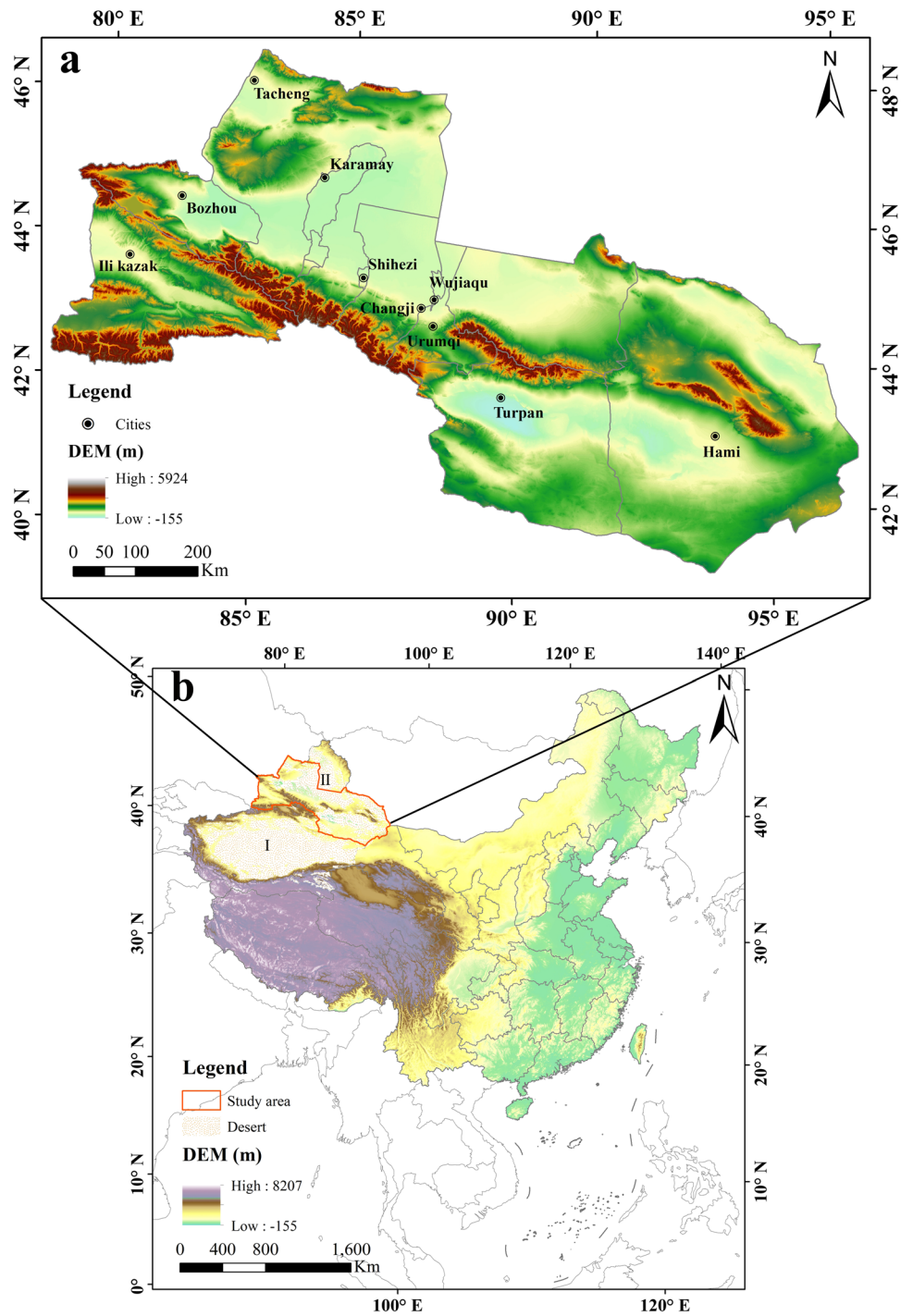
PSCF and CWT method

The potential source contribution function (PSCF) method is a method developed to qualitatively identify potential sources of pollution based on a conditional probability function. By combining the trajectory of an air mass with the value of an element (e.g., the hourly concentration of a pollutant) corresponding to that trajectory, PSCF is frequently used to identify potential source areas of high concentrations of pollutants affecting receptor sites. A higher value indicates that the grid cell has a higher probability of being a potential source area causing air pollution in the target city. The calculation formula is as follows (Nicolas et al. 2011; Wang et al. 2009a, b):

$$\text{PSCF}_{ij} = \frac{m_{ij}}{n_{ij}} \quad (1)$$

where PSCF_{ij} is the ratio of the trajectory endpoints m_{ij} exceeding the threshold criterion to all trajectory endpoints n_{ij} in grid ij . To reduce the effect of small values of n_{ij} in the

Fig. 1 Location of the study area. The DEM data (Shuttle Radar Topography Mission, SRTM) were downloaded from the Geospatial Data Cloud (<http://www.gscloud.cn/>) and processed using ArcGIS 10.2 software. **a** Map of China and location map of the Xinjiang deserts provided by National Tibetan Plateau Data Center (<http://data.tpdc.ac.cn/>): I. Taklimakan Desert, II. Gurbantungut Desert. **b** Enlarged topographic map of NSTM



grid cells, multiply W_{ij} (the weight function) by the PSCF value as follows:

$$WPSCF_{ij} = PSCF_{ij} \times W_{ij} \tag{2}$$

$$W_{ij} = \begin{cases} 1.00, & n_{ij} > 80 \\ 0.70, & 80 \geq n_{ij} > 20 \\ 0.42, & 20 \geq n_{ij} > 10 \\ 0.05, & 10 \geq n_{ij} \end{cases} \tag{3}$$

The PSCF method cannot distinguish between cases where the trajectory corresponds to a concentration slightly above the threshold or much above the threshold. Therefore, this deficiency is compensated by combining CWT, which can quantitatively reflect the pollution level of the different trajectories. Higher values of CWT indicate a

greater likelihood that the potential source will contribute to high pollution levels at the target cell, as follows (Hsu et al. 2003; Dimitriou and Kassomenos 2015):

$$CWT_{ij} = \frac{1}{\sum_{l=1}^M \tau_{ijl}} \sum_{l=1}^M C_l \tau_{ijl} \tag{4}$$

$$WCWT_{ij} = CWT_{ij} \times W_{ij} \tag{5}$$

where CWT_{ij} is the average weighted concentration of cell grid ij , M is the total number of trajectories, τ_{ijl} is the time that trajectory l stays on grid ij , and C_l is the concentration of trajectory l when it passes through grid ij . As with PSCF, W_{ij} is introduced to reflect the uncertainty of the values in each grid cell. The resolution of each grid cell in the PSCF

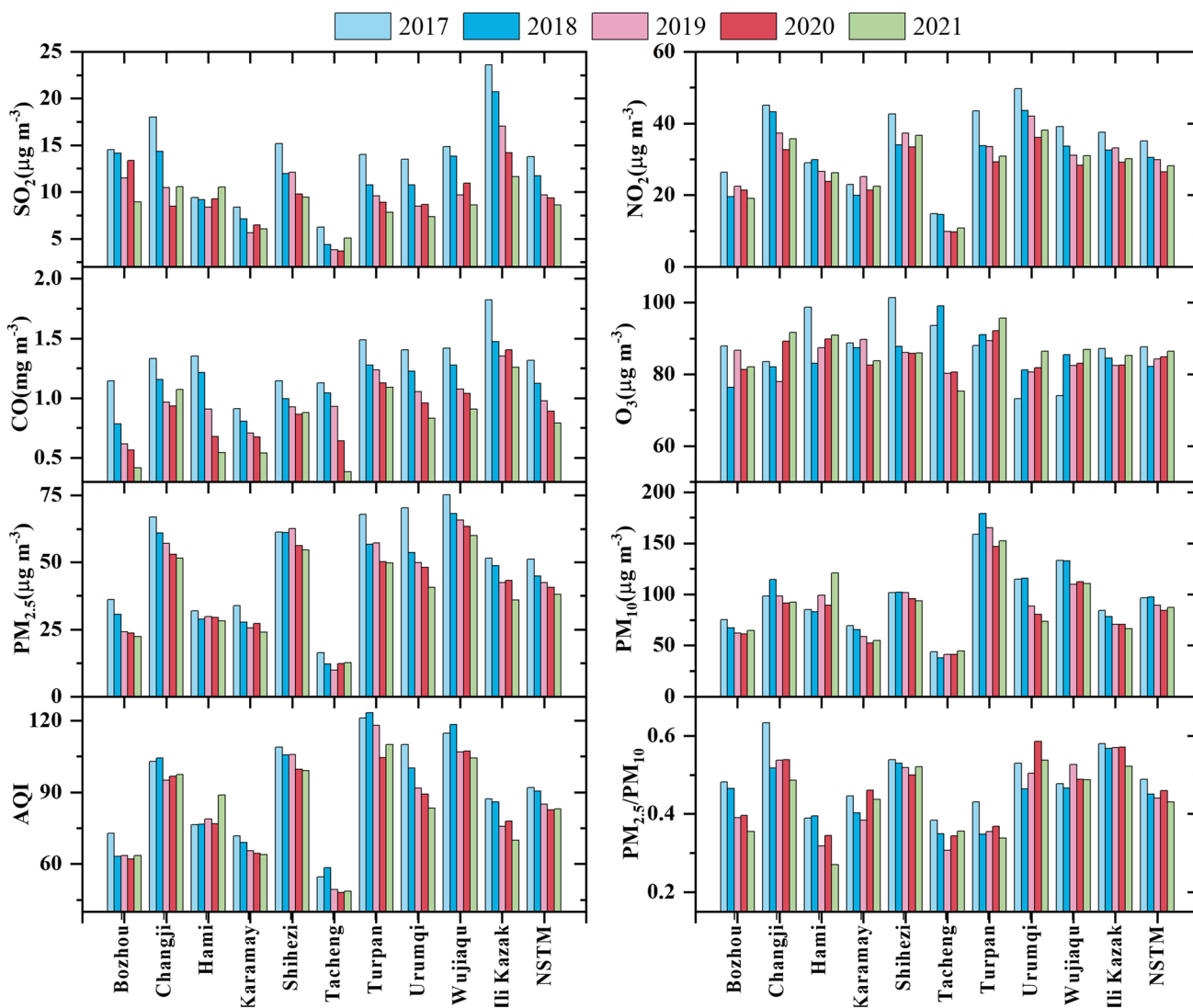


Fig. 2 Average values of concentrations of air pollutants during 2017–2021 in the NSTM region

and CWT methods is $0.5^\circ \times 0.5^\circ$, and the $PM_{2.5}$ and PM_{10} criteria were set to 75 and $150 \mu\text{g m}^{-3}$ in the PSCF analysis according to the NAAQS Grade II.

Results and discussion

Characteristics of air pollutants

Spatio-temporal characteristics of the air pollutants

The 5-year averages (Table S3) and year-to-year pollutant concentration variations (Fig. 2) were shown in the NSTM and each city (January 2017–December 2021). The annual mean concentrations of SO_2 , NO_2 , CO, O_3 , $PM_{2.5}$, and PM_{10} in the NSTM region ranged from 8.61 to $13.76 \mu\text{g m}^{-3}$, 26.53– $36.06 \mu\text{g m}^{-3}$, 0.79– 1.31mg m^{-3} , 84.29– $87.62 \mu\text{g m}^{-3}$, 37.98– $51.10 \mu\text{g m}^{-3}$, and 84.15– $97.47 \mu\text{g m}^{-3}$, respectively. Except for O_3 , the concentrations of SO_2 , NO_2 , CO, $PM_{2.5}$, and PM_{10} exhibited a decreasing trend from 2017 to 2021, at an average rate of -1.265 , -1.779 , -0.128 , -3.042 , and -3.135 per year, respectively, while the concentration of O_3 showed a slight increasing trend (at an average rate of 1.90% per year), and the trends of pollutants in the NSTM and the cities are shown in Table S4. The significant decreases in the annual average concentrations of pollutants (except O_3) were attributed to specific environmental protection efforts. Among them, the concentrations of NO_2 , $PM_{2.5}$, and PM_{10} in Urumqi decreased by 23.10%, 42.25%, and 36.11% in 2021 compared to 2017, respectively, with the largest decreasing trends (-3.047 , -6.496 , and $-11.828 \mu\text{g m}^{-3} \text{year}^{-1}$), indicating that the governmental regulation of air quality in the NSTM was initiated from Urumqi, especially for more effective control of particulate matter. The increase in O_3 concentration was associated with VOCs and NO_x (nitrogen oxides) formation from vehicle exhaust, as well as the reduction of $PM_{2.5}$ and NO_2 , which was beneficial to O_3 formation (Li et al. 2018b; Liu et al. 2020). In addition, the annual mean concentrations of NO_2 and PM_{10} in 2020 were lower than in 2021, which is associated with a significant reduction in urban traffic due to the stagnation of production activities caused by COVID-19 (Wang et al. 2020c). Rupakheti et al. (2021) had done air pollutants characterization research throughout Xinjiang, and the results showed a slight decreasing trend in the concentrations of SO_2 , CO, and $PM_{2.5}$ from 2015 to 2018, while the concentrations of NO_2 , O_3 , and PM_{10} showed an increasing trend. To more clearly compare the changes over a long period of time, we added concentrations of air pollutants in 2015 and 2016. From 2015 to 2021 (Fig. S1), SO_2 concentrations have been decreasing; NO_2 , CO, $PM_{2.5}$, and PM_{10} show an increasing trend followed by a decreasing trend; and O_3 concentrations

show an increasing trend. The comparison found that the trend in the NSTM from 2015 to 2018 was generally consistent with the whole of Xinjiang. The NO_2/SO_2 ratio is a crucial indicator for identifying whether the air pollutant originates from stationary (e.g., industrial emissions) or fuel-powered mobile sources (Aneja et al. 2001). The higher NO_2/SO_2 ratio indicates a greater contribution to air pollution from mobile sources, primarily from motor vehicle emissions (Song et al. 2017). The Yangtze River Delta, Huai River, Chengdu–Chongqing, and the Pearl River Delta NO_2/SO_2 ratios were higher in the pre-2020 period with 9.07, 7.40, 7.14, and 6.69, respectively (Bai et al. 2022). Due to the economic reliance on transportation in these high-tech industrialized urban agglomerations, mobile sources produce more air pollution than stationary sources (Zhao et al. 2018a; Song et al. 2017). While a relatively low ratio of 2.82 was observed in this study, this was due to the fact that the cities in the NSTM region were resource-based cities with an aggregation of heavy industries, and thus stationary source emissions such as coal and biomass burning, which were the primary factors restricting air quality (Turap et al. 2019).

Among the ten cities in the NSTM, the lowest annual average SO_2 , NO_2 , $PM_{2.5}$, and PM_{10} concentrations were observed in Tacheng, with values of $4.63 \mu\text{g m}^{-3}$, $11.96 \mu\text{g m}^{-3}$, $12.65 \mu\text{g m}^{-3}$, and $41.71 \mu\text{g m}^{-3}$, respectively. Tacheng's northernmost distant and sparsely populated location (area: 4356km^2 , population: 1.14 million, CAR PARC: 0.36 million, <http://www.xjtc.gov.cn/info/2727/183468.htm>) in the NSTM was the reason for the lowest concentrations of pollutants there. The highest annual average SO_2 and CO concentrations were found in Ili Kazak, with values of $17.44 \mu\text{g m}^{-3}$ and 1.46mg m^{-3} , due to the typical coal-smoke air pollution in Ili Kazak (Zhong et al. 2022), where the main source of coal-smoke pollution is coal combustion and the main pollutants are SO_2 , CO, and smoke, in addition to NO_x . The highest annual average concentrations of NO_2 ($41.91 \mu\text{g m}^{-3}$), $PM_{2.5}$ ($66.52 \mu\text{g m}^{-3}$), and PM_{10} ($160.57 \mu\text{g m}^{-3}$) were observed in Urumqi, Wujiaqu, and Turpan, respectively. The highest concentrations of NO_2 were found over Urumqi, an economic and political center with more anthropogenic activities than other places, and high NO_2 values were mainly caused by NO_x from traffic-related sources. Notably, according to the Chinese NAAQS annual average $PM_{2.5}$ concentration threshold of $35 \mu\text{g m}^{-3}$, the 5-year average $PM_{2.5}$ concentrations in Shihezi and Wujiaqu were $59.23 \mu\text{g m}^{-3}$ (69.23% exceedance) and $66.52 \mu\text{g m}^{-3}$ (90.01% exceedance), which even exceeded the Beijing–Tianjin–Hebei $PM_{2.5}$ concentration of $57.98 \mu\text{g m}^{-3}$ in 2015–2019 (Luo et al. 2022). Moreover, the concentration of PM_{10} in Turpan significantly exceeded the NAAQS guideline. This indicated that the particulate matter pollution in the NSTM was extremely serious, and more attention should be paid to air pollution in this area.

The average AQI in the NSTM from 2017 to 2021 was 86.61, which reached the national secondary standard. This result included 67 and 290 yearly average days that met the primary and secondary standards, respectively, accounting for 18.41% and 61.32% of the total number of days. Over the past 5 years, the annual mean AQI has been 91.98, 90.44, 85.04, 82.70, and 82.91, respectively, indicating an improving trend in ambient air quality in the NSTM. Tacheng exhibited the lowest annual average AQI of 51.77 ± 3.99 , with the lowest annual mean value of 48.04 in 2020. However, the annual average AQI of Turpan, Wujiaqu, and Shihezi were 115.38 ± 7.04 , 110.27 ± 5.28 , and 103.73 ± 3.81 , respectively, with an annual average of 45.8, 24.2, and 58.2 days of heavily polluted weather, indicating that the three cities suffered from severe pollution. Turpan was severely affected by sand and dust, especially during the spring, when PM_{10} concentration even exceeded $2000 \mu\text{g m}^{-3}$ and AQI reached the upper limit (with a value of 500). The pollution in Wujiaqu and Shihezi was particularly severe in winter, when the rate of heavy pollution (AQI > 200) was as high as 57.21%

and 46.12%, respectively, so the government should implement appropriate air quality improvement measures according to the pollution characteristics of each city.

$PM_{2.5}/PM_{10}$ ratios can identify different source approaches and processes of formation (Blanco-Becerra et al. 2015). Low $PM_{2.5}/PM_{10}$ indicated that natural processes associated with sand particles were primarily responsible for air pollution (Abuelgasim and Farahat 2020), whereas high ratios were associated with NO_3^- , SO_4^{2-} , NH_4^+ , and organic matter, which are secondary particles generated (Chan et al. 2005). For all of China, the ratio was 0.59 (Song et al. 2017), but the ratio was much higher in megacities such as Beijing, Shanghai, and Guangzhou, even exceeding 0.7 (Wang et al. 2014b), indicating a major contribution of finer anthropogenic particles (Xu et al. 2017). With a decreasing interannual variation, the mean $PM_{2.5}/PM_{10}$ ratio in the NSTM was 0.45 ± 0.02 ; higher ratios were found in Ili Kazakh, Urumqi, and Shihezi (0.56 ± 0.02 , 0.52 ± 0.04 , and 0.52 ± 0.01 , respectively), while lower ratios were found in Hami, Tacheng, and Turpan (0.34 ± 0.05 , 0.35 ± 0.02 , and

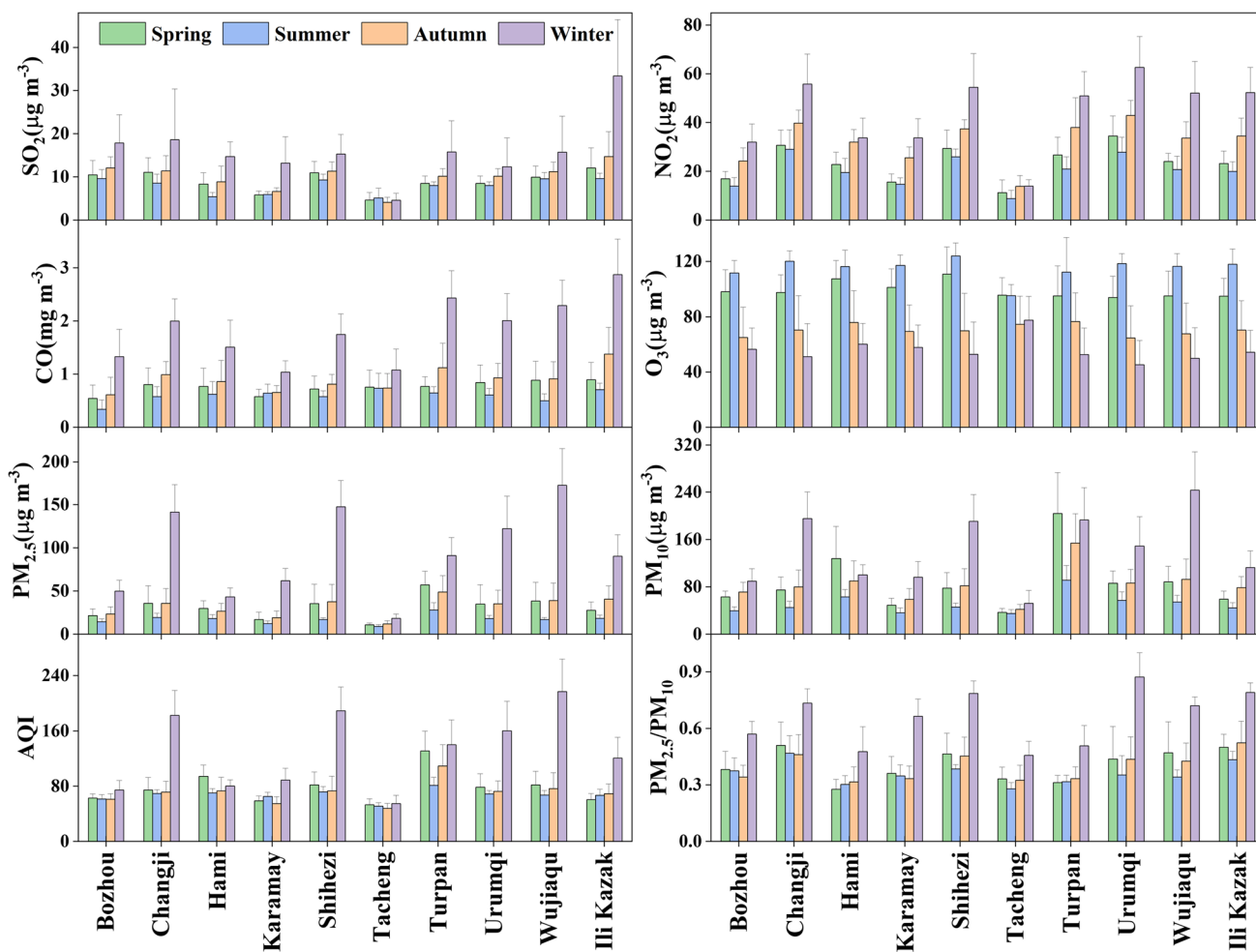


Fig. 3 Seasonal characteristics of concentrations of air pollutants from 2017 to 2021

0.37 ± 0.03 , respectively). Apart from the above, the lowest $PM_{2.5}/PM_{10}$ ratio of 0.27 was observed in Hami in 2021, while the highest value of 0.63 was found in Changji in 2017. During the 5 years of the study, the NSTM's $PM_{2.5}/PM_{10}$ ratio was lower than that of the majority of Chinese cities. The atmosphere was more impacted by coarse particulate matter, indicating that the NSTM is vulnerable to sandstorms in the Taklamakan and Gurbantunggut Deserts.

Seasonal variations

Figure 3 shows seasonal fluctuations in air pollution concentrations over various cities in the NSTM. Winter > autumn > spring > summer was the order of the seasonal variation of SO_2 , NO_2 , and CO concentration values in almost all cities. Summer had the lowest SO_2 , NO_2 , and CO concentrations, which ranged from $5.13 \pm 2.25 \mu\text{g m}^{-3}$ (Tacheng) to $9.65 \pm 2.09 \mu\text{g m}^{-3}$ (Bozhou), $8.85 \pm 3.37 \mu\text{g m}^{-3}$ (Tacheng) to $29.13 \pm 7.88 \mu\text{g m}^{-3}$ (Changji), and $0.34 \pm 0.18 \text{mg m}^{-3}$ (Bozhou) to $0.73 \pm 0.28 \text{mg m}^{-3}$ (Tacheng). Accordingly, winter was the season with the highest SO_2 , NO_2 , and CO concentrations, ranging from $4.62 \pm 1.57 \mu\text{g m}^{-3}$ (Tacheng) to $33.37 \pm 13.06 \mu\text{g m}^{-3}$ (Ili Kazak), $13.89 \pm 2.68 \mu\text{g m}^{-3}$ (Tacheng) to $62.60 \pm 12.72 \mu\text{g m}^{-3}$ (Urumqi), and $1.08 \pm 0.39 \text{mg m}^{-3}$ (Tacheng) to $2.87 \pm 0.67 \text{mg m}^{-3}$ (Ili Kazak). The highest concentration of NO_2 in Urumqi was due to relatively high human activity and coal burning in winter, while the lowest values were found in Tacheng with minor anthropogenic activities. The combined impacts of primary emissions from domestic heating, adverse diffusion circumstances, and photochemical processes were responsible for this outcome (Zhao et al. 2015). However, the trend for O_3 was the opposite of the above, with the seasonal order of concentrations being summer > spring > autumn > winter. Similar findings in China were obtained by Li et al. (2019). The mean O_3 concentration during summer ranged from $95.35 \pm 8.05 \mu\text{g m}^{-3}$ (Tacheng) to $124.04 \pm 9.47 \mu\text{g m}^{-3}$ (Shihezi), while in winter, the concentrations ranged from $45.25 \pm 17.62 \mu\text{g m}^{-3}$ (Urumqi) to $77.60 \pm 17.23 \mu\text{g m}^{-3}$ (Tacheng). This was primarily caused by the intense solar radiation, high temperatures, and potent photochemical processes that characterize summer, all of which favor the creation of O_3 .

For almost all of the cities, the concentrations of $PM_{2.5}$ and PM_{10} were highest in the winter and lowest in the summer. However, Hami and Turpan were found to have the highest PM_{10} concentrations in the spring season, which may be frequently influenced by dust storms and floating dust. The highest $PM_{2.5}$ concentration occurred in Wujiaqu in winter ($172.79 \pm 42.48 \mu\text{g m}^{-3}$) and the lowest in Tacheng in summer ($9.21 \pm 1.96 \mu\text{g m}^{-3}$), with a ratio of up to 19 times between them. Similarly for PM_{10} , the value in Wujiaqu in winter was 7 times higher than that in Tacheng in summer.

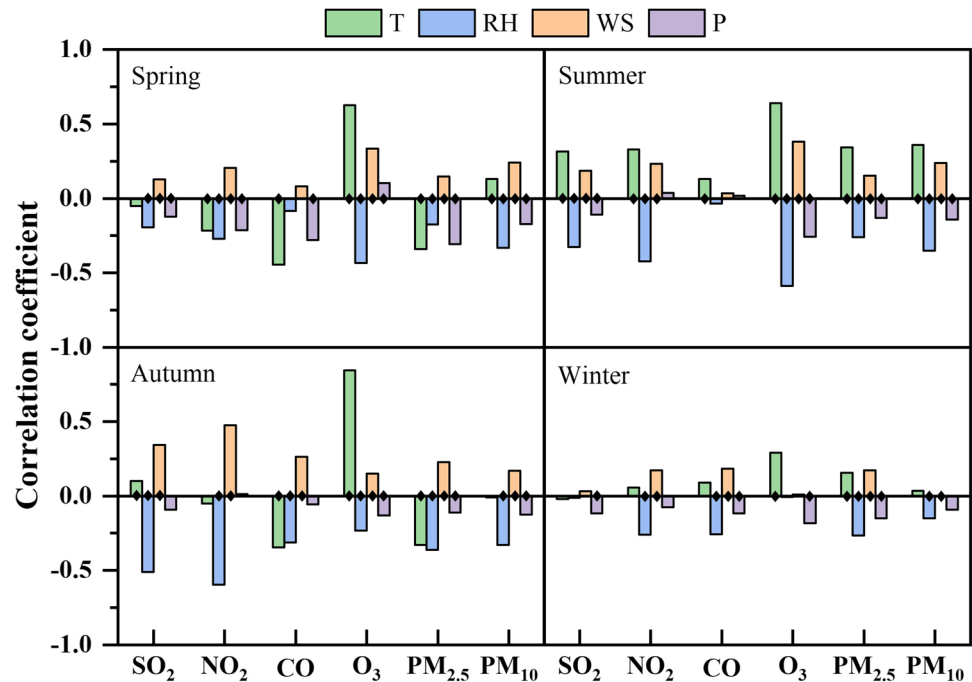
That was mainly caused by the use of large quantities of coal for heating, poor weather conditions, and a significant rise in traffic over the Chinese New Year, all of which can lead to a rise in the accumulation of particulate matter and pollution events during winter.

Seasonal mean AQI values ranged from 67.42 ± 7.27 (summer) to 130.84 ± 52.78 (winter) in the study area, indicating that the air quality was markedly better in summer than in winter. Due to the high density of heavy industry in the NSTM region and the massive amount of coal that will be used for heating in the winter, the pollution levels are quite high. The total amount of pollutant emissions exceeds the local environmental capacity during the winter due to decreased environmental capacity, worsening diffusion conditions, and the addition of unfavorable meteorological conditions. In summer, there was no coal consumption for central heating, although coal consumption for power generation was also higher, due to stronger airflow convection and more precipitation, resulting in lower pollutant concentrations. As a result, air quality is worse in winter than in summer. The highest AQI value was found in the winter in Wujiaqu (216.98 ± 47.21), while the lowest AQI value was found in the autumn in Tacheng (47.90 ± 7.43). However, the values for Hami were higher in spring, and this difference can be attributed to the impact of coarse particles brought by dust storms. Seasonal mean $PM_{2.5}/PM_{10}$ ratios ranged from 0.36 ± 0.05 (summer) to 0.66 ± 0.14 (winter) in the study area. The $PM_{2.5}/PM_{10}$ ratios showed the highest ratios in winter, which was associated with anthropogenic pollution, with the highest value occurring in Urumqi (0.87 ± 0.13), followed by Ili Kazak and Shihezi with values of 0.79 ± 0.05 and 0.79 ± 0.07 , while lower rates were observed in spring and summer in Hami (0.28 ± 0.05 , 0.30 ± 0.05), Tacheng (0.33 ± 0.06 , 0.28 ± 0.03), and Turpan (0.31 ± 0.04 , 0.32 ± 0.03). That was caused by significant emissions of coarse particulate matter from sandy and wasteland areas as well as the frequent dust storms in semi-desert and desert regions of northwest China (Zou and Zhai 2004; Zhang and Cao 2015; Song et al. 2017).

Influence of meteorological conditions

Concentrations of air pollutants depend primarily on the influence of meteorological conditions when local emissions are relatively stable (Li et al. 2012). Qi et al. (2021) found that the influence of individual meteorological factors on concentrations of air pollutants was limited, while a combination of meteorological factors was more effective. Due to the availability of data, Urumqi, the capital of Xinjiang province, was chosen as a representative to analyze the relationship between pollutant concentrations and meteorological conditions. The meteorological factors include daily

Fig. 4 Correlation coefficient of meteorological factors and concentrations of air pollutants by season (diamond shape indicates $p < 0.05$)



temperature (T), relative humidity (RH), wind speed (WS), wind direction (WD), and pressure (P).

Pearson correlation coefficients between the main meteorological factors and concentrations of air pollutants (Fig. 4) were calculated using SPSS (Guo et al. 2019). The correlations between pollutant concentrations and meteorological factors varied significantly with the seasons, with the smallest correlation in winter, which was due to the high concentrations of pollutants (except O₃) in winter that were also associated with pollution emissions, topography, etc. In all seasons, temperature and O₃ showed a significant positive correlation, with high temperatures and solar radiation favoring the formation of O₃ in the atmosphere. Wind speed exhibited a positive correlation with concentrations of air pollutants, because an increase in wind speed under unique geographic conditions and wind direction led to the accumulation of concentrations of pollutants. In addition, relative humidity showed a negative correlation with concentrations of air pollutants, and the correlation between air pressure and concentrations of pollutants was minimal. We performed the analysis of temperature, relative humidity, wind speed, and wind direction to learn more about the meteorological factors that influence air pollutants (Figs. 5 and 6).

NO₂, CO, and PM_{2.5} were found to be significantly negatively correlated with temperature, and atmospheric convection can be found to play an important role in their concentration regulation. Under high-temperature conditions, strong turbulence and other thermal activities of the atmosphere accelerate their diffusion (Yang et al. 2016a, b), and conversely, low temperatures weaken atmospheric convection and enhance their accumulation (Chen et al.

2020; Li et al. 2015, 2014). The highest concentrations of NO₂, CO, and PM_{2.5} were reached at temperatures of -13 to -6 °C rather than at the lowest temperatures (Fig. 5). Due to the lower surface temperatures in winter, an increase in temperature might cause a temperature inversion layer to form that would prevent atmospheric motion and result in an accumulation of pollutants (Xu et al. 2019). SO₂ and PM₁₀ concentrations showed a slightly negative correlation with temperature. Similarly, at temperatures between -13 and -6 °C, the maximum concentration of PM₁₀ ($> 300 \mu\text{g m}^{-3}$) was recorded, but the SO₂ concentration remained lower ($< 50 \mu\text{g m}^{-3}$, below the NAAQS Grade I). O₃ showed a strong positive correlation with temperature. When the temperature exceeds 15 °C, the concentration of O₃ can reach more than $100 \mu\text{g m}^{-3}$, and some even exceed the NAAQS Grade II ($> 160 \mu\text{g m}^{-3}$). The same results as Atkinson (2000) were obtained that high temperatures and low humidity favor the formation of O₃. Pollutants were all slightly negatively correlated with RH. The highest mass concentrations were found at 30–50% RH, which could be attributed to the surge of pollutants emitted by centralized heating and the suppression of the atmospheric boundary layer during the winter. Humidity greater than 80% was concentrated in March, April, May, and October, when pollutants were more easily dispersed due to higher wind speeds. In addition, as the relative humidity rises, suspended particles assemble and become heavy enough to enable both dry deposition (particle drop) and wet deposition (precipitation) (Li et al. 2015).

Wind speed plays a vital role in the concentration of pollutants. Wind can enhance the flow of the atmosphere, which promotes the diffusion, dilution, and transmission of

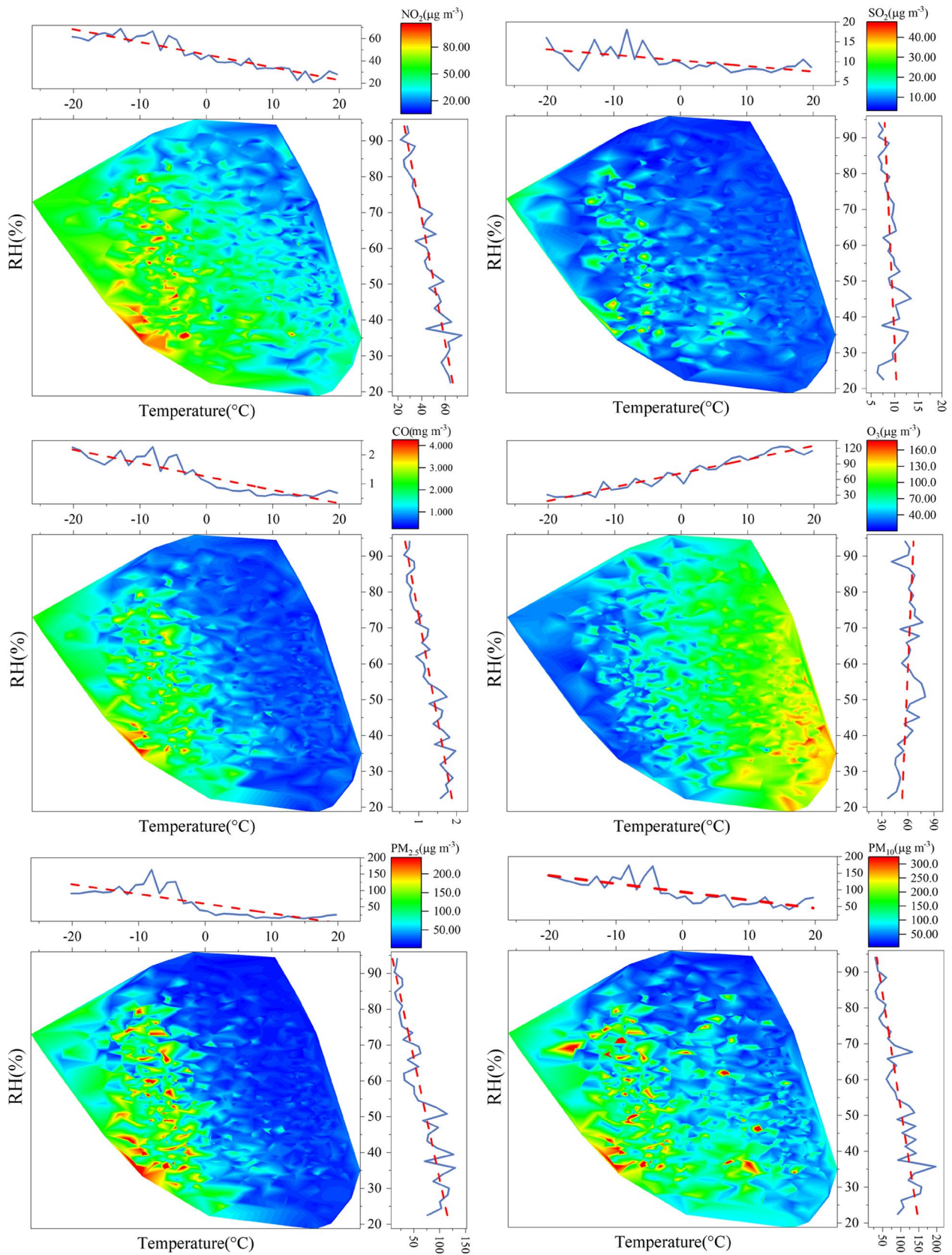
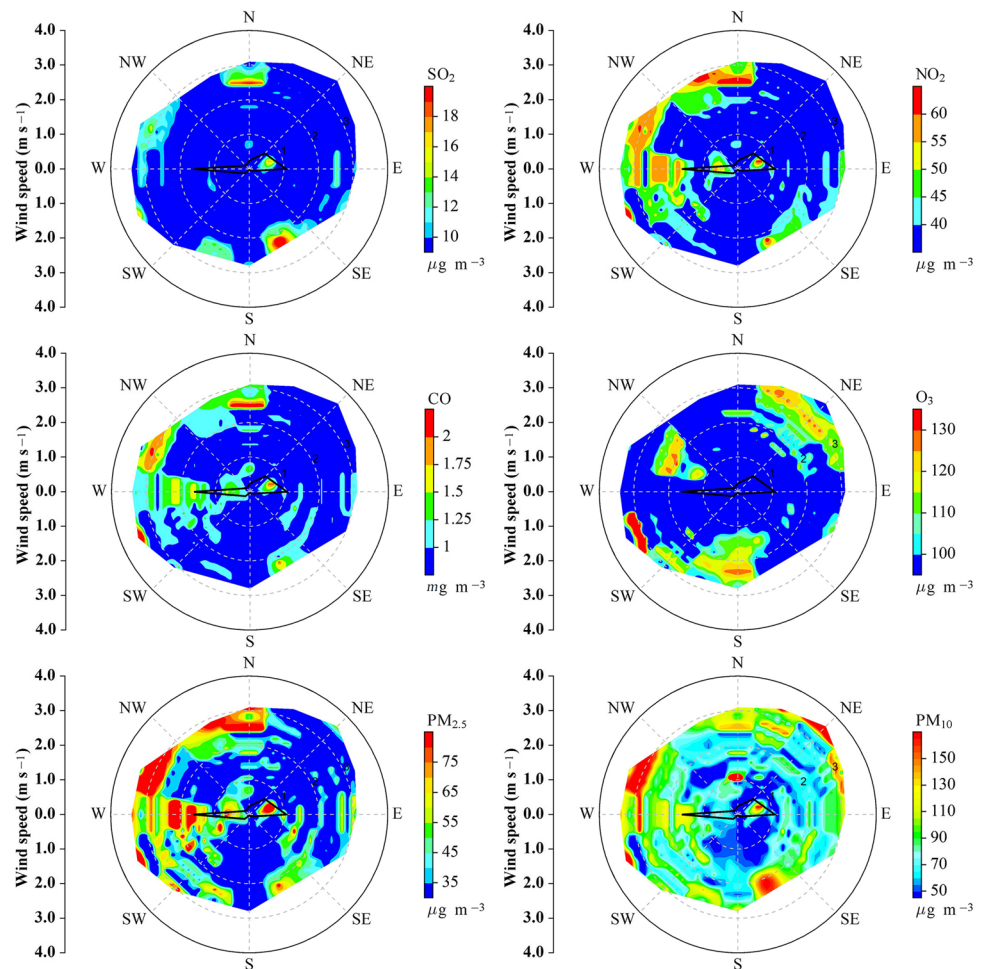


Fig. 5 Relationship between concentrations of six air pollutants and meteorological factors

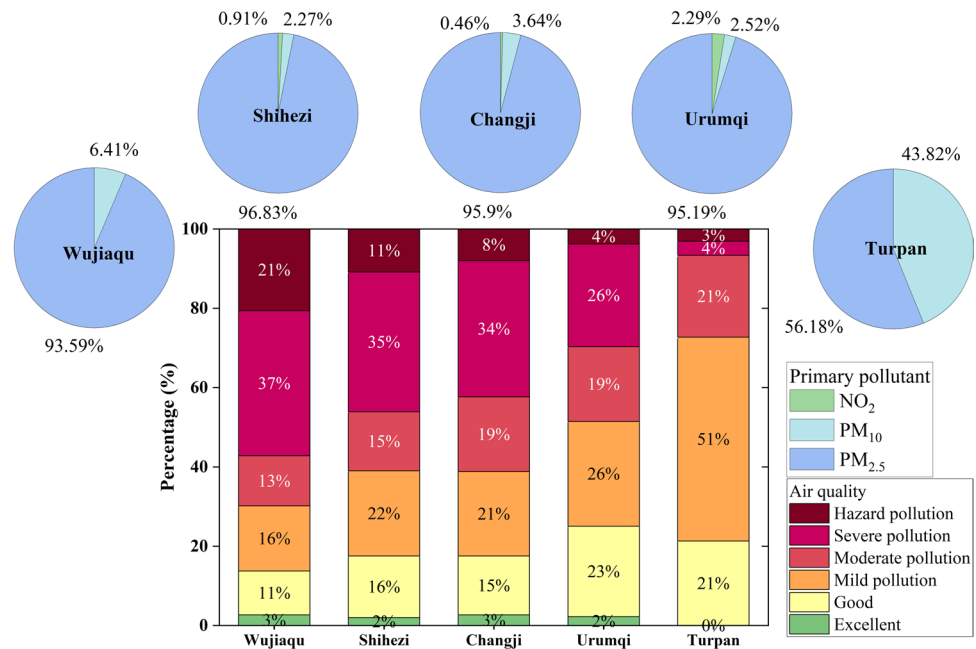
Fig. 6 Windrose of six air pollutants



pollutants, effectively lowering their concentration. As seen in Fig. 4, the correlations between wind speed and concentrations of air pollutants were weak, indicating that concentrations of pollutants may be more closely related to wind direction than wind speed, which determines the source of pollution. In order to better understand the effect of wind direction and wind speed on concentrations of air pollutants, they were analyzed with the support of the wind rose diagram (Fig. 6). It demonstrated that the northeast and west winds are mostly responsible for the high concentrations of SO_2 , NO_2 , and CO when the wind speed is less than 2 m s^{-1} . When the wind speed was more than 2 m s^{-1} , the north winds were followed by the northwest, southeast, and west winds as the directions with the highest SO_2 , NO_2 , and CO concentrations. The highest O_3 concentrations were primarily from the northwest and south winds when the wind speed was less than 3 m s^{-1} ; while the wind speed was greater than 3 m s^{-1} , the highest O_3 concentrations were primarily from the southwest wind, followed by the northeast wind. The

$\text{PM}_{2.5}$ concentrations were higher in the east wind at all wind speeds. In addition, high $\text{PM}_{2.5}$ concentrations ($> 75 \mu\text{g m}^{-3}$) also came from the northwest, north, and southwest winds at high wind speeds. The results suggest that the concentrations of air pollutants may be mainly influenced by local emissions and external transport. West winds were correlated with higher concentrations of NO_2 , CO , and $\text{PM}_{2.5}$, which may be brought about by massive industrial emissions and frequent human activities in the western economic development zones and may also be transmitted from Changji and Shihezi upward in the west. High PM_{10} concentrations ($> 150 \mu\text{g m}^{-3}$, exceeding NAAQS Grade II) were mainly associated with high wind speeds, mainly from the northwest, northeast, and southeast winds. Furthermore, at various wind speeds, PM_{10} concentrations mostly exceeded the NAAQS Grade I ($50 \mu\text{g m}^{-3}$). It indicated that the local PM_{10} was mainly transported regionally and that the pollution was more serious.

Fig. 7 Air quality conditions and primary pollutants in heavily polluted cities



Transport path and potential sources of particulate matter

Backward trajectory analysis during winter

The backward trajectory and cluster analysis reveal the transport paths of air masses reaching Wujiacqu, Shihezi, Changji, Urumqi, and Turpan, where particulate matter concentrations exceed NAAQS Grade II and air quality is poor in winter (Fig. 7). The distributions of the backward trajectory cluster in these five cities over the winter are shown in Fig. 8. Using MeteoInfo software, trajectories from the winter of 2017–2021 were classified according to the speed and direction of their transmission. Furthermore, a total of 1804 trajectories were obtained for each city, and the multiple trajectories were divided into four clusters. To account for the impact of each pathway on air quality in the five cities, the average pollutant concentration for each cluster can be calculated using the cluster statistics function of MeteoInfo’s trajStat plug-in.

In Wujiacqu, 60.09% of the air masses (clusters 1 and 4) originated in eastern Kazakhstan and then traveled via Ili Kazak. 22.45% (cluster 2) originated in Tacheng, passed through the southern Karamay and Changji, arrived in eastern Urumqi, and then turned around to head toward Wujiacqu after being obstructed by the Tianshan Mountains. Cluster 3 (17.46%) mainly came from northeastern Kazakhstan via northeastern Tacheng. Cluster 2 in Wujiacqu contained the highest PM_{2.5} (196.4 μg m⁻³) and PM₁₀ (281.24 μg m⁻³) concentrations (Fig. 9), indicating that the cluster contributes significantly to the PM_{2.5} and PM₁₀ concentrations in Wujiacqu. It showed that regional environmental cooperation

should be strengthened, and joint prevention and control measures for air pollution should be implemented. The second highest concentrations were in cluster 1, with PM_{2.5} and PM₁₀ concentrations as high as 192.58 μg m⁻³ and 270.58 μg m⁻³, respectively. With high pollution levels in Wujiacqu, it demonstrated that particulate matter was still a significant air pollutant to be concerned about.

In Shihezi, air clusters were mainly from the west, with a total of 75.88% (cluster 2 and cluster 1). Cluster 2 (39.41%) originated in eastern Kazakhstan and passed through Ili Kazak, Tacheng, and Changji. Cluster 1 from near the Ili River accounted for 36.74%, then crossed Tacheng and Karamay. Among them, clusters 1 and 2 were interspersed in the northern part of Ili Kazak. Cluster 3 originated in the eastern part of Tacheng, and Cluster 4 was from the north of Changji and local emissions, accounting for 14.69% and 9.42%, respectively. With 153.86 μg m⁻³ of PM_{2.5}, Cluster 2 had the highest concentration. Clusters 1 and 3 corresponded to PM_{2.5} concentrations of 147.38 μg m⁻³ and 147.26 μg m⁻³, respectively, indicating that the areas through which the airflow passes play an essential role in the PM_{2.5} concentration in Shihezi. Cluster 4, of which the trajectories made up only 9.42% of all trajectories, contained the highest PM₁₀ concentration (204.79 μg m⁻³). The above indicated that the surrounding areas contribute significantly to the concentration of PM₁₀.

In Changji, clusters 1, 2, and 4 all originated in eastern Kazakhstan, with contributions of 46.18%, 12.20%, and 27.55% to the total trajectories (totally accounting for 85.93%). Clusters 1 and 2 were two trajectories of different speeds, passing through Ili Kazak and south of

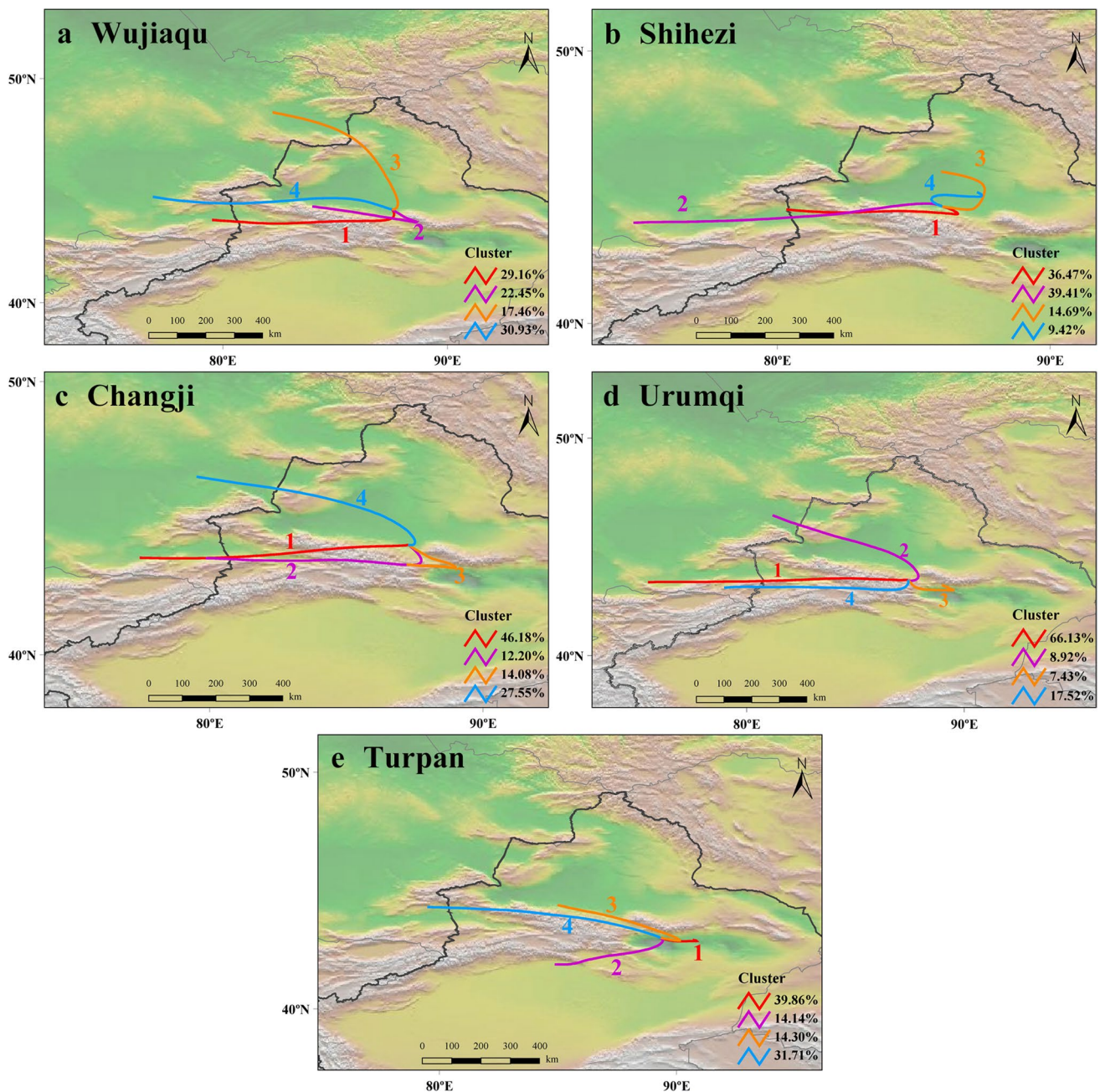


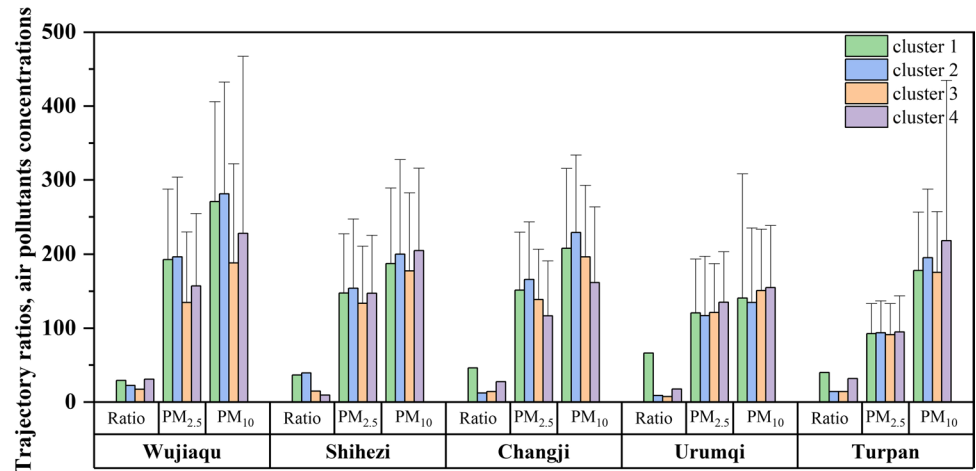
Fig. 8 The trajectories of heavily polluted cities in winter

Tacheng. Cluster 4 crossed central Tacheng and Karamay. 14.08% of the total trajectories (cluster 3) were from the surrounding areas of Changji, which crossed Urumqi and Turpan. Cluster 2 contained the highest $PM_{2.5}$ concentrations ($165.87 \mu g m^{-3}$) and the highest PM_{10} concentrations ($228.88 \mu g m^{-3}$). Cluster 1 contained the second highest concentrations of $PM_{2.5}$ and PM_{10} ($151.28 \mu g m^{-3}$ and $207.94 \mu g m^{-3}$, respectively). The results showed that eastern Kazakhstan, Ili Kazakh, and Tacheng were the most

crucial transport pathways affecting the concentrations of particulate matter in Changji in winter.

In Urumqi, the trajectories of clusters 1, 2, and 4 were similar to those of clusters 1, 4, and 2 in Changji, accounting for 66.13%, 8.92%, and 17.52%, respectively, adding up to 92.57% of all trajectories from eastern Kazakhstan. Unlike the Changji trajectories, cluster 3 (7.43%) originated from the Turpan Basin. Compared to the other four cities, Urumqi showed the slightest difference in particulate matter

Fig. 9 Trajectory ratios and PM concentrations of each trajectory cluster



concentrations between the four clusters, with PM_{2.5} (PM₁₀) concentrations ranging from 116 to 135 $\mu\text{g m}^{-3}$ (134 to 154 $\mu\text{g m}^{-3}$). It showed that eastern Kazakhstan, Ili Kazak, and southern Changji were the most influential transmission pathways for particulate matter concentrations in Urumqi in winter.

In Turpan, the backward trajectories mainly originated from local emissions. Cluster 1 represented the main trajectory, which accounts for 39.86% of the total trajectories. Besides, the airflow was dominated by the northwest direction. Cluster 4 (31.71%) originated in eastern Kazakhstan and passed through Ili Kazak, Bozhou, Tacheng, Changji, and Urumqi. 14.30% (cluster 3) came from Karamay and across Tacheng, Changji, and Urumqi. 14.14% of the total trajectories (cluster 2) were from the north of the Taklamakan Desert. With a mean concentration of 93.19 $\mu\text{g m}^{-3}$ across all four clusters, PM_{2.5} concentrations ranged from 92 to 95 $\mu\text{g m}^{-3}$. The highest PM₁₀ concentrations were found in clusters 4 and 2, with values of 217.79 $\mu\text{g m}^{-3}$ and 195.07 $\mu\text{g m}^{-3}$, respectively. The desert, which could deliver sand and dust to Turpan, was the source of these two clusters. Thus, the concentration values of PM₁₀ were higher.

It is worth noting that all five cities have clusters originating in eastern Kazakhstan and have a significant share of the total trajectories. In order to supply heavy industry, there were coal mines in eastern Kazakhstan. The two primary industrial sectors that produce the majority of emissions are electricity generation and metallurgy. The eastern cities of Almaty and Ust-Kamenogorsk were the two cities with the highest monthly average concentrations of pollutants in 2019 (Assanov et al. 2021a), where the severe pollution in Ust-Kamenogorsk was not primarily caused by transport but rather by large industrial and power plants (Assanov et al. 2021b). And the two biggest coal-fired power plants were located in Ekibastuz in the northeast, indicating that the NSTM also received regional air pollutants from its borders. However, due to the long distance of the trajectories

from Kazakhstan and greater air mass speed, the probability of pollution transfer was reduced, and the issue of pollution probability will be specified in the subsequent PSCF and CWT analyses. Furthermore, the shorter air clusters suggested that the air masses flowed slowly and that pollutants were ready to accumulate (Yu et al. 2019). The shorter clusters of these five cities' clusters are as follows: cluster 2 in Wujiaqu, clusters 3 and 4 in Shihezi, cluster 3 in Changji, cluster 3 in Urumqi, and cluster 1 in Turpan. The observation was attributed to heavy local emissions along with natural sources of atmospheric pollutants.

Potential sources of particulate matter

The backward trajectory model can be used to identify the paths that air masses travel during transport, but it cannot be used to quantify the contribution of potential sources that could affect particulate matter. Therefore, to determine the potential regions, we employed the CWT and PSCF methods. The findings of the weighted potential source contribution function (WPSCF) and weighted concentration weighted trajectory (WCWT) maps for PM_{2.5} and PM₁₀ in Wujiaqu (a), Shihezi (b), Changji (c), Urumqi (d), and Turpan (e) are shown in Figs. 9 and 10.

High WPSCF scores (Fig. 10) suggest potential source areas for severe pollution in the corresponding regions. During the winter period in Wujiaqu, the distribution and morphology of potential contribution sources of PM_{2.5} and PM₁₀ were similar, except that the potential contribution sources of PM_{2.5} corresponded to higher WPSCF values. The junction of Turpan, Urumqi, Changji, Tacheng, Ili Kazak, and Bayingol Mongolian Autonomous Prefecture (hereinafter Bayingol Mongolian) corresponds to the area of higher WPSCF values for PM_{2.5} (WPSCF > 0.9) and PM₁₀ (WPSCF > 0.8). For Shihezi, the regions with high WPSCF values for PM_{2.5} (WPSCF > 0.9) and PM₁₀ (WPSCF > 0.8) were similar, mainly in northeastern Aksu, northwest of

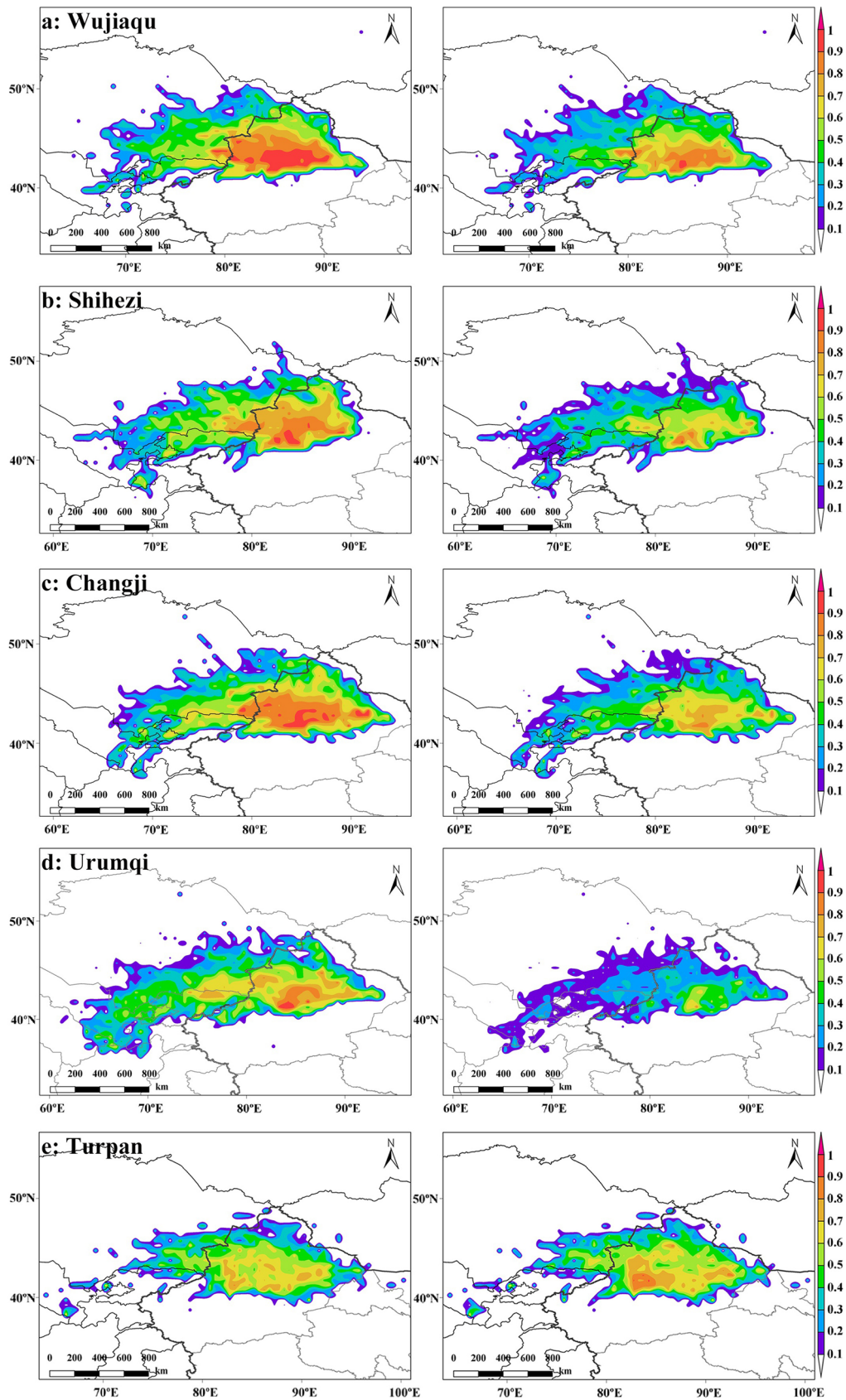


Fig. 10 PSCF maps of particulate matter in winter (The left graphs depict $PM_{2.5}$, while the right graphs depict PM_{10})

Turpan, and the junction of Aksu and Bayingol Mongolian. Compared to $PM_{2.5}$, the area of high-value WPSCF was reduced for PM_{10} . For Changji, the Bayingol Mongolian's southern region and the intersection of Hami and Turpan had the highest concentrations of $PM_{2.5}$ WPSCF values, which were more than 0.9. Besides, areas with high WPSCF values were discovered along Ili Kazak and in the southeast of Kazakhstan, which were in the path of leading clusters 1 and 2 of higher $PM_{2.5}$ concentrations (151.28 – $165.87 \mu\text{g m}^{-3}$). This was associated with Almaty, a large heavy industry city in southeast Kazakhstan, which had one of the highest annual average concentrations of total suspended particulate matter and also had the largest population and transport vehicles (Assanov et al. 2021a, b). Northwestern Bayingol Mongolian was the main potential contribution source for PM_{10} , with a WPSCF value higher than 0.8. For Urumqi, the intersection of Aksu and Bayingol Mongolian had the highest PSCF values for $PM_{2.5}$ (WPSCF > 0.9). The WPSF values for PM_{10} were generally not high, and higher values (WPSCF > 0.5) were found in northern Bayingol Mongolian. For Turpan, the WPSCF values for $PM_{2.5}$ were higher than 0.7, mainly in the eastern of Aksu, the northern of Bayingol Mongolian, Turpan local emission, and the junction of Urumqi, Changji, and Bayingol Mongolian. As for PM_{10} , the primary potential sources (WPSCF > 0.8) in Turpan were western Hami, the junction of Aksu, and Bayingol Mongolian. Due to its long-distance migration, the Taklamakan Desert region was one of the main potential contributors to both $PM_{2.5}$ and PM_{10} in Turpan, which was associated with the contribution of sandstorms (Wang et al. 2015).

The PSCF method can only account for the contribution rate of the potential source area and cannot distinguish between trajectory concentrations that are slightly above the threshold and those that are substantially above the threshold. Therefore, CWT is utilized to determine the weight concentration of trajectories to remedy this deficiency and to reflect the pollution level of different trajectories quantitatively (Fig. 11).

In Wujiaqu, the higher WCWT values for $PM_{2.5}$ and PM_{10} were distributed in the same regions, Urumqi, northwestern Turpan, northern Bayingol Mongolian, and Ili Kazak, where $PM_{2.5} > 200 \mu\text{g m}^{-3}$ and $PM_{10} > 280 \mu\text{g m}^{-3}$ were found. In Shihezi, the high WCWT values of $PM_{2.5}$ ($> 270 \mu\text{g m}^{-3}$) were located at the intersection of Aksu and Bayingol Mongolian, while high WCWT values of PM_{10} ($> 200 \mu\text{g m}^{-3}$) were distributed in northeastern Aksu and southwestern Changji. In Changji, the region of high WCWT values for $PM_{2.5}$ ($> 100 \mu\text{g m}^{-3}$) was similar to the area corresponding to WPSCF > 0.5, covering almost the entire study area and southeastern Kazakhstan. The area of high PM_{10} WCWT was also wide, with NSTM, northeastern Aksu, and northwestern Bayingol Mongolian contributing to $PM_{10} > 200 \mu\text{g m}^{-3}$. In Urumqi, the regions of high WCWT

values of $PM_{2.5}$ (WCWT > $140 \mu\text{g m}^{-3}$) were similar to the regions with high WPSCF values (WPSCF > 0.8). In addition, the highest WCWT values ($> 200 \mu\text{g m}^{-3}$) were found in the intersection of northeast Urumqi and Changji. The highest WCWT values for PM_{10} were positioned in western Bozhou and central Tacheng, where cluster 2 (PM_{10} concentration of $134.66 \mu\text{g m}^{-3}$) passes through the highest WCWT value area. In Turpan, the potential source areas with high WCWT values of $PM_{2.5}$ were in general agreement with the results of WPSCF. The high WCWT values ($> 100 \mu\text{g m}^{-3}$) were distributed in the Aksu, Turpan, and Bayingol Mongolian. The areas with the highest PM_{10} WCWT ($> 210 \mu\text{g m}^{-3}$) were the Urumqi–Changji–Shihezi region, southeast Changji, and the junction of northwest Bayingol Mongolian and southeast Ili Kazak. The results indicated that regional pollution transport could significantly impact the air quality in the study area.

Conclusion

The characteristics of six criteria pollutants, influence of major meteorological factors on concentrations of air pollutants, and potential source regions of particulate matter in heavily polluted cities were investigated for the NSTM. The concentrations of air pollutants (SO_2 , NO_2 , CO, PM_{10} , and $PM_{2.5}$) showed a downward trend from 2017 to 2021, while the opposite was observed for O_3 . The highest concentrations of air pollutants (apart from O_3) were found in winter, especially in Wujiaqu, Shihezi, Changji, Urumqi, and Turpan, where the particulate matter concentrations exceed NAAQS Grade II. Temperature showed a significant negative correlation with concentrations of air pollutants (excluding O_3), and relative humidity showed a weak negative correlation to air pollutants, which may be related to the deposition due to increased humidity. High concentrations of pollutants were more influenced by the west wind, which was related to the emission of pollutants from local economic development zones and the transmission of pollutants from the Changji–Shihezi region. At higher wind speeds, the high concentration of coarse particles was more associated with the long-distance transmission of sand and dust. The results of PSCF and CWT indicated that the WPSCF values of $PM_{2.5}$ were higher in heavily polluted regions during winter, which was mainly influenced by centralized heating and unfavorable diffusion conditions, while the WPSCF values of PM_{10} were larger in Turpan, indicating that sandstorms have more influence on it. The potential source areas were mainly distributed in Urumqi–Changji–Shihezi, Turpan, the northern Bayingol Mongolian, and eastern Kazakhstan. The next step aims to combine local emission data for a more comprehensive source analysis of pollutants. In general, air quality improvement should be based on reducing local

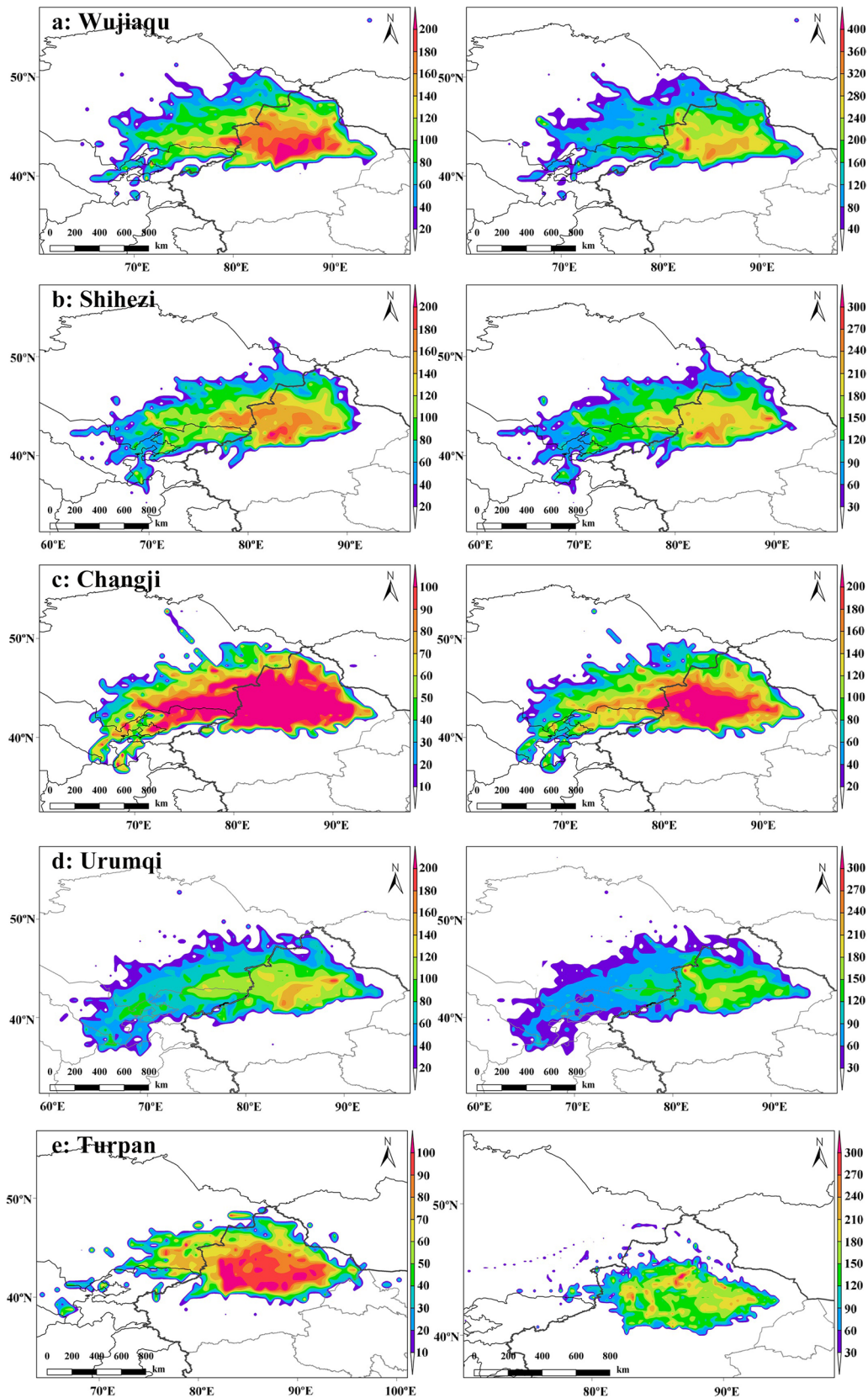


Fig. 11 CWT maps of particulate matter in winter (The left graphs depict $PM_{2.5}$, while the right graphs depict PM_{10} . Unit: $\mu g m^{-3}$)

emissions, strengthening regional cooperation, and researching transboundary transport of air pollutants.

Supplementary Information The online version contains supplementary material available at <https://doi.org/10.1007/s11356-023-25757-4>.

Author contribution YL: conceptualization, methodology, writing—original draft. LX and ZL: conceptualization, supervision. XZ: conceptualization, supervision, writing—review and editing. XZ and FW: methodology, writing—review and editing. JP and CC: review and editing. ZC and HY: investigation, data curation.

Funding This work was supported by Third Xinjiang Scientific Expedition (TXSE) program (2022xjkk0101; 2021xjkk1401), The Second Tibetan Plateau Scientific Expedition and Research (2019QZKK0201), the Strategic Priority Research Program of Chinese Academy of Sciences (Class A)(XDA20060201;XDA20020102), The SKLCS founding (SKLCS-ZZ-2022), and the National Natural Science Foundation of China (41471058).

Data availability All data are taken from publicly available sources, and the datasets generated for this study are available from the corresponding author upon reasonable request.

Declarations

Ethical approval Not applicable.

Consent to participate Not applicable.

Consent for publication The authors certify that the manuscript is our original, unpublished work and is not under consideration by another journal. All authors have approved the manuscript and agree with its submission.

Competing interests The authors declare no competing interests.

References

- Abuelgasim A, Farahat A (2020) Investigations on PM₁₀, PM_{2.5}, and their ratio over the Emirate of Abu Dhabi. *United Arab Emirates Earth Syst Environ* 4:763–775. <https://doi.org/10.1007/s41748-020-00186-2>
- Aneja VP, Agarwal A, Roelle PA, Phillips SB, Tong Q, Watkins N (2001) Measurements and analysis of criteria pollutants in New Delhi, India. *Environ Int* 27(1):35–42. [https://doi.org/10.1016/S0160-4120\(01\)00051-4](https://doi.org/10.1016/S0160-4120(01)00051-4)
- Assanov D, Kerimray A, Batkeyev B, Kapsalyamova Z (2021) The effects of COVID-19-related driving restrictions on air quality in an industrial city. *Aerosol Air Qual Res* 21:200663. <https://doi.org/10.4209/aaqr.200663>
- Assanov D, Zapasnyi V, Kerimray A (2021b) Air quality and industrial emissions in the cities of Kazakhstan. *Atmos* 12:314. <https://doi.org/10.3390/atmos12030314>
- Atkinson R (2000) Atmospheric chemistry of VOCs and NOx. *Atmos Environ* 34:2063–2101. [https://doi.org/10.1016/S1352-2310\(99\)00460-4](https://doi.org/10.1016/S1352-2310(99)00460-4)
- Bai YT, Wang ZC, Xie F, Cen L, Xie ZL, Zhou XJ et al (2022) Changes in stoichiometric characteristics of ambient air pollutants pre- to post-COVID-19 in China. *Environ Res* 209:112806. <https://doi.org/10.1016/j.envres.2022.112806>
- Blanco-Becerra LC, Gáfarro-Rojas AI, Rojas-Roa NY (2015) Influence of precipitation scavenging on the PM_{2.5}/PM₁₀ ratio at the Kennedy locality of Bogota, Colombia. *Rev Fac Ing Univ Antioq* 76:58–65. <https://doi.org/10.17533/udea.redin.n76a07>
- Cao JS, Li WH, Tan JG, Song WM, Xu XH, Jiang C et al (2009) Association of ambient air pollution with hospital outpatient and emergency room visits in Shanghai, China. *Sci Total Environ* 407(21):5531–5536. <https://doi.org/10.1016/j.scitotenv.2009.07.021>
- Chan CY, Xu XD, Li YS, Wong KH, Ding GA, Chan LY et al (2005) Characteristics of vertical profiles and sources of PM_{2.5}, PM₁₀ and carbonaceous species in Beijing. *Atmos Environ* 39(28):5113–5124. <https://doi.org/10.1016/j.atmosenv.2005.05.009>
- Chen RJ, Chu C, Tan JG, Cao JS, Song WM, Xu XH et al (2010) Ambient air pollution and hospital admission in Shanghai, China. *J Hazard Mater* 181:234–240. <https://doi.org/10.1016/j.jhazmat.2010.05.002>
- Chen ZY, Chen DL, Zhao CF, Kwan M, Cai J, Zhuang Y et al (2020) Influence of meteorological conditions on PM_{2.5} concentrations across China: a review of methodology and mechanism. *Environ Int* 139:105558. <https://doi.org/10.1016/j.envint.2020.105558>
- Cohen AJ, Brauer M, Burnett R, Anderson HR, Frostad J, Estep K et al (2017) Estimates and 25-year trends of the global burden of disease attributable to ambient air pollution: an analysis of data from the Global Burden of Diseases Study 2015. *Lancet* 389:1907–1918. [https://doi.org/10.1016/S0140-6736\(17\)30505-6](https://doi.org/10.1016/S0140-6736(17)30505-6)
- Development and Reform Commission of Xinjiang Uygur Autonomous Region (2017) Main functional zone plan of Xinjiang Uygur Autonomous Region. [WWW Document]. <http://xjdrx.xinjiang.gov.cn/xjfgw/c108377/201712/15e792086bfe4465934806790b2dda2.shtml>. Accessed 2 Jan 2023
- Dimitriou K, Kassomenos P (2015) Three-year study of tropospheric ozone with back trajectories at a metropolitan and a medium scale urban area in Greece. *Sci Total Environ* 502:493–501. <https://doi.org/10.1016/j.scitotenv.2014.09.072>
- Draxler RR, Rolph GD (2003) HYSPLIT (Hybrid Single-Particle Lagrangian Integrated Trajectory) Model access via NOAA ARL READY. NOAA Air Resources Laboratory, Silver Spring, MD. <http://www.arl.noaa.gov/ready/hysplit>. Accessed 2 Jan 2023
- Fan H, Zhao CF, Yang YK (2020) A comprehensive analysis of the spatio-temporal variation of urban air pollution in China during 2014–2018. *Atmos Environ* 220:117066. <https://doi.org/10.1016/j.atmosenv.2019.117066>
- Fang CL (2019) Strategic thinking and spatial layout for the sustainable development of urban agglomeration in northern slope of Tianshan Mountains. *Ganhanqu dili* 42:1–11. <https://doi.org/10.12118/j.issn.1000-6060.2019.01.01>. in Chinese
- Geng GN, Xiao QY, Zheng YX, Tong D, Zhang YX, Zhang XY et al (2019) Impact of China's air pollution prevention and control action plan on PM_{2.5} chemical composition over eastern China. *Sci China Earth Sci* 62:1872–1884. <https://doi.org/10.1007/s11430-018-9353-x>
- Geng GN, Zheng YX, Zhang Q, Xue T, Zhao HY, Tong D et al (2021) Drivers of PM_{2.5} air pollution deaths in China 2002–2017. *Nat Geosci* 14:645–650. <https://doi.org/10.1038/s41561-021-00792-3>
- Guo H, Gu XF, Ma GX, Shi SY, Wang WN, Zuo X et al (2019) Spatial and temporal variations of air quality and six air pollutants in China during 2015–2017. *Sci Rep* 9:15201. <https://doi.org/10.1038/s41598-019-50655-6>
- Han LJ (2018) Relationship between urbanization and urban air quality: an insight on fine particulate dynamics in China. *Dili kexue jinzhan* 37(08):1011–1021. <https://doi.org/10.18306/dlkxjz.2018.08.001>. in Chinese
- He JJ, Gong SL, Yu Y, Yu LJ, Wu L, Mao HJ et al (2017) Air pollution characteristics and their relation to meteorological conditions during 2014–2015 in major Chinese cities. *Environ Pollut* 223:484–496. <https://doi.org/10.1016/j.envpol.2017.01.050>

- Hsu YK, Holsen TM, Hopke PK (2003) Comparison of hybrid receptor models to locate PCB sources in Chicago. *Atmos Environ* 37(4):545–562. [https://doi.org/10.1016/S1352-2310\(02\)00886-5](https://doi.org/10.1016/S1352-2310(02)00886-5)
- Hu JL, Wang YG, Ying Q, Zhang HL (2014) Spatial and temporal variability of PM_{2.5} and PM₁₀ over the North China Plain and the Yangtze River Delta, China. *Atmos Environ* 95:598–609. <https://doi.org/10.1016/j.atmosenv.2014.07.019>
- Jhun I, Coull BA, Schwartz J, Hubbell B, Koutrakis P (2015) The impact of weather changes on air quality and health in the United States in 1994–2012. *Environ Res Lett* 10:084009. <https://doi.org/10.1088/1748-9326/10/8/084009>
- Kan HD, Chen RJ, Tong SL (2012) Ambient air pollution, climate change, and population health in China. *Environ Int* 42:10–19. <https://doi.org/10.1016/j.envint.2011.03.003>
- Kang HQ, Zhu B, Van der Alvarez RJ, Zhu CM, de Leeuw G, Hou XW et al (2019) Natural and anthropogenic contributions to long-term variations of SO₂, NO₂, CO, and AOD over East China. *Atmos Res* 215:284–293. <https://doi.org/10.1016/j.atmosres.2018.09.012>
- Leibensperger EM, Mickley LJ, Jacob DJ, Barrett SRH (2011) Intercontinental influence of NO_x and CO emissions on particulate matter air quality. *Atmos Environ* 45(19):3318–3324. <https://doi.org/10.1016/j.atmosenv.2011.02.023>
- Li YY, Dai J (2022) Construction and implementation approaches of ecological compensation mechanism for coordinated control of air pollution in Beijing–Tianjin–Hebei Region. *Meteorol Environ Res* 13(1):43–48. <https://doi.org/10.19547/j.issn2152-3940.2022.01.011>
- Li XF, Zhang MJ, Wang SJ, Zhao AF, Ma Q (2012) Variation characteristics and influencing factors of air pollution index in China. *Environ Sci* 33(6):1936–1943. <https://doi.org/10.13227/j.hjxx.2012.06.035>. in Chinese
- Li L, Huang C, Huang HY, Wang YJ, Yan RS, Zhang GF et al (2014) An integrated process rate analysis of a regional fine particulate matter episode over Yangtze River Delta in 2010. *Atmos Environ* 91:60–70. <https://doi.org/10.1016/j.atmosenv.2014.03.053>
- Li J, Chen HB, Li ZQ, Wang PC, Cribb M, Fan XH (2015) Low-level temperature inversions and their effect on aerosol condensation nuclei concentrations under different large-scale synoptic circulations. *Adv Atmos Sci* 32(7):898–908. <https://doi.org/10.1007/s00376-014-4150-z>
- Li HJ, Zhou DQ, Wei YJ (2018) An assessment of PM_{2.5}-related health risks and associated economic losses in Chinese cities. *Huanjing Kexue* 39(8):3467–3475. <https://doi.org/10.13227/j.hjxx.20171237>. in Chinese
- Li K, Jacob DJ, Liao H, Shen L, Zhang Q, Bates KH (2018b) Anthropogenic drivers of 2013–2017 trends in summer surface ozone in China. *Proc Natl Acad Sci USA* 116(2):422–427. <https://doi.org/10.1073/pnas.1812168116>
- Li R, Wang ZZ, Cui LL, Fu HB, Zhang LW, Kong LD et al (2019) Air pollution characteristics in China during 2015–2016: Spatiotemporal variations and key meteorological factors. *Sci Total Environ* 648:902–915. <https://doi.org/10.1016/j.scitotenv.2018.08.181>
- Liu L, Zhang ZY, Liu F, Xu LP (2018) Spatial-temporal distribution and simulation analysis of PM_{2.5} concentration of the cities in the northern slope economic zone of Tianshan Mountain. *Res Environ Sci* 31(11):1849–1857. <https://doi.org/10.13198/j.issn.1001-6929.2018.07.15>. in Chinese
- Liu YS, Zhou Y, Lu JX (2020) Exploring the relationship between air pollution and meteorological conditions in China under environmental governance. *Sci Rep* 10(1):14518. <https://doi.org/10.1038/s41598-020-71338-7>
- Luo YH, Zhao TL, Yang YJ, Zong L, Kumar KR, Wang H et al (2022) Seasonal changes in the recent decline of combined high PM_{2.5} and O₃ pollution and associated chemical and meteorological drivers in the Beijing–Tianjin–Hebei region, China. *Sci Total Environ* 838:156312. <https://doi.org/10.1016/j.scitotenv.2022.156312>
- Ma XY, Jia HL, Sha T, An JL, Tian R (2019) Spatial and seasonal characteristics of particulate matter and gaseous pollution in China: implications for control policy. *Environ Pollut* 248:421–428. <https://doi.org/10.1016/j.envpol.2019.02.038>
- Ma W, Ding JL, Wang R, Wang JL (2022) Drivers of PM_{2.5} in the urban agglomeration on the northern slope of the Tianshan Mountains, China. *Environ Pollut* 309:119777. <https://doi.org/10.1016/j.envpol.2022.119777>
- Nicolás J, Chiari M, Crespo J, Galindo N, Lucarelli F, Nava S et al (2011) Assessment of potential source regions of PM_{2.5} components at a southwestern Mediterranean site. *Tellus Ser B Chem phys meteorol* 63(1):96–106. <https://doi.org/10.1111/j.1600-0889.2010.00510.x>
- Qi J, Zheng B, Li M, Yu F, Chen CC, Liu F et al (2017) A high-resolution air pollutants emission inventory in 2013 for the Beijing–Tianjin–Hebei region, China. *Atmos Environ* 170:156–168. <https://doi.org/10.1016/j.atmosenv.2017.09.039>
- Qi XY, Mei G, Cuomo S, Liu C, Xu NX (2021) Data analysis and mining of the correlations between meteorological conditions and air quality: a case study in Beijing. *Internet of Things* 14:100127. <https://doi.org/10.1016/j.iot.2019.100127>
- Rupakheti D, Yin XF, Rupakheti M, Zhang QG, Li P, Rai M et al (2021) Spatio-temporal characteristics of air pollutants over Xinjiang, northwestern China. *Environ Pollut* 268:115907. <https://doi.org/10.1016/j.envpol.2020.115907>
- Shen Y, Zhang LP, Fang X, Ji HY, Li X, Zhao ZW (2019) Spatiotemporal patterns of recent PM_{2.5} concentrations over typical urban agglomerations in China. *Sci Total Environ* 655:13–26. <https://doi.org/10.1016/j.scitotenv.2018.11.105>
- Song CB, Wu L, Xie YC, He JJ, Chen X, Wang T et al (2017) Air pollution in China: status and spatiotemporal variations. *Environ Pollut* 227:334–347. <https://doi.org/10.1016/j.envpol.2017.04.075>
- Tian YL, Jiang Y, Liu Q, Xu DX, Zhao SD, He LH et al (2019) Temporal and spatial trends in air quality in Beijing. *Landsc Urban Plan* 185:35–43. <https://doi.org/10.1016/j.landurbplan.2019.01.006>
- Turap Y, Talifu D, Wang XM, Abulizi A, Maihemuti M, Tursun Y et al (2019) Temporal distribution and source apportionment of PM_{2.5} chemical composition in Xinjiang, NW-China. *Atmos Res* 218:257–268. <https://doi.org/10.1016/j.atmosres.2018.12.010>
- Wang YQ (2014) MeteorInfo: GIS software for meteorological data visualization and analysis. *Meteorol Appl* 21(2):360–368. <https://doi.org/10.1002/met.1345>
- Wang K, Zhang Y, Jang C, Phillips S, Wang BY (2009) Modeling intercontinental air pollution transport over the trans-Pacific region in 2001 using the Community Multiscale Air Quality modeling system. *J Geophys Res Atmos* 114:04307. <https://doi.org/10.1029/2008jd010807>
- Wang YQ, Zhang XY, Draxler RR (2009b) TrajStat: GIS-based software that uses various trajectory statistical analysis methods to identify potential sources from long-term air pollution measurement data. *Environ Model Softw* 24(8):38–939. <https://doi.org/10.1016/j.envsoft.2009.01.004>
- Wang SJ, Zhang MJ, Minguillón MC, Zhang XY, Feng F, Qiu X (2014a) PM₁₀ concentration in urban atmosphere around the eastern Tien Shan, Central Asia during 2007–2013. *Environ Sci Pollut Res* 22:6864–6876. <https://doi.org/10.1007/s11356-014-3911-7>
- Wang YG, Ying Q, Hu JL, Zhang HL (2014b) Spatial and temporal variations of six criteria air pollutants in 31 provincial capital cities in China during 2013–2014. *Environ Int* 73:413–422. <https://doi.org/10.1016/j.envint.2014.08.016>
- Wang LL, Liu ZR, Sun Y, Ji DS, Wang YS (2015) Long-range transport and regional sources of PM_{2.5} in Beijing based on long-term observations from 2005 to 2010. *Atmos Res* 157:37–48. <https://doi.org/10.1016/j.atmosres.2014.12.003>

- Wang XY, Dickinson RE, Su LY, Zhou CL, Wang KC (2018) PM_{2.5} pollution in China and how it has been exacerbated by terrain and meteorological conditions. *Bull Am Meteorol Soc* 99:105–119. <https://doi.org/10.1175/BAMS-D-16-0301.1>
- Wang YH, Gao WK, Wan S, Song T, Gong ZY, Ji DS et al (2020a) Contrasting trends of PM_{2.5} and surface ozone concentrations in China from 2013 to 2017. *Natl Sci Rev* 7(8):1331–1339. <https://doi.org/10.1093/nsr/nwaa032>
- Wang PF, Chen KY, Zhu SQ, Wang P, Zhang HL (2020c) Severe air pollution events not avoided by reduced anthropogenic activities during COVID-19 outbreak. *Resources Conserv Recycl* 158:104814. <https://doi.org/10.1016/j.resconrec.2020.104814>
- Wang W, Samat A, Abuduwaili J, Ge YX (2020b) Spatio-temporal variations of satellite-based PM_{2.5} concentrations and its determinants in Xinjiang, northwest of China. *Int J Environ Res Public Health* 17(6):2157. <https://doi.org/10.3390/ijerph17062157>
- Wang FL, Li ZQ, Wang FT, You XN, Xia DS, Zhang X et al (2021) Air pollution in a low-industry city in China's silk road economic belt: characteristics and potential sources. *Front Earth Sci* 9:527475. <https://doi.org/10.3389/feart.2021.527475>
- Xu G, Jiao LM, Zhang BE, Zhao SL, Yuan M, Gu YY et al (2017) Spatial and temporal variability of the PM_{2.5}/PM₁₀ ratio in Wuhan, Central China. *Aerosol Air Qual Res* 17(3):741–751. <https://doi.org/10.4209/aaqr.2016.09.0406>
- Xu TT, Song Y, Liu MX, Cai XH, Zhang HS, Guo JP et al (2019) Temperature inversions in severe polluted days derived from radio-sonde data in North China from 2011 to 2016. *Sci Total Environ* 647:1011–1020. <https://doi.org/10.1016/j.scitotenv.2018.08.088>
- Yang X, Zhao CF, Zhou LJ, Wang Y, Liu XH (2016a) Distinct impact of different types of aerosols on surface solar radiation in China. *J Geophys Res Atmos* 121(11):6459–6471. <https://doi.org/10.1002/2016jd024938>
- Yang Y, Liao H, Lou SJ (2016) Increase in winter haze over eastern China in recent decades: Roles of variations in meteorological parameters and anthropogenic emissions. *J Geophys Res Atmos* 121(21):13,050–13,065. <https://doi.org/10.1002/2016jd025136>
- Yin P, Brauer M, Cohen AJ, Wang HD, Li J, Burnett RT et al (2020) The effect of air pollution on deaths, disease burden, and life expectancy across China and its provinces, 1990–2017: an analysis for the Global Burden of Disease Study 2017. *Lancet Planet Health* 4(9):e386–e398. [https://doi.org/10.1016/s2542-5196\(20\)30161-3](https://doi.org/10.1016/s2542-5196(20)30161-3)
- Yin XF, Kang SC, Rupakheti M, de Foy B, Li P, Yang JH et al (2021) Influence of transboundary air pollution on air quality in south-western China. *Geosci Front* 12(6):101239. <https://doi.org/10.1016/j.gsf.2021.101239>
- Yu H, Yang W, Wang XH, Yin BH, Zhang X, Wang J et al (2019) A seriously sand storm mixed air-polluted area in the margin of Tarim Basin: Temporal-spatial distribution and potential sources. *Sci Total Environ* 676:436–446. <https://doi.org/10.1016/j.scitotenv.2019.04.298>
- Yuan Q, Qi B, Hu DY, Wang JJ, Zhang J, Yang HQ et al (2021) Spatiotemporal variations and reduction of air pollutants during the COVID-19 pandemic in a megacity of Yangtze River Delta in China. *Sci Total Environ* 751:141820. <https://doi.org/10.1016/j.scitotenv.2020.141820>
- Zhang YL, Cao F (2015) Fine particulate matter (PM 2.5) in China at a city level. *Sci Rep* 5:14884. <https://doi.org/10.1038/srep14884>
- Zhang HL, Wang YG, Hu JL, Ying Q, Hu XM (2015) Relationships between meteorological parameters and criteria air pollutants in three megacities in China. *Environ Res* 140:242–254. <https://doi.org/10.1016/j.envres.2015.04.004>
- Zhang QQ, Ma Q, Zhao B, Liu XY, Wang YX, Jia BX et al (2018) Winter haze over North China Plain from 2009 to 2016: Influence of emission and meteorology. *Environ Pollut* 242:1308–1318. <https://doi.org/10.1016/j.envpol.2018.08.019>
- Zhang Q, Zheng YX, Tong D, Shao M, Wang SX, Zhang YH et al (2019) Drivers of improved PM_{2.5} air quality in China from 2013 to 2017. *Proc Natl Acad Sci* 116(49):24463–24469. <https://doi.org/10.1073/pnas.1907956116>
- Zhao SP, Yu Y, Yin DY, He JJ (2015) Meteorological dependence of particle number concentrations in an urban area of complex terrain, Northwestern China. *Atmos Res* 164:304–317. <https://doi.org/10.1016/j.atmosres.2015.06.001>
- Zhao DT, Chen H, Li XD, Ma XT (2018a) Air pollution and its influential factors in China's hot spots. *J Clean Prod* 185:619–627. <https://doi.org/10.1016/j.jclepro.2018.02.181>
- Zhao SP, Yu Y, Yin DY, Qin DH, He JJ, Dong LX (2018b) Spatial patterns and temporal variations of six criteria air pollutants during 2015 to 2017 in the city clusters of Sichuan Basin, China. *Sci Total Environ* 624:540–557. <https://doi.org/10.1016/j.scitotenv.2017.12.172>
- Zhong YT, Li X, Fan ZA, Ayitken M, Li ST, Liu XC (2022) Chemical composition characteristics and source contributions of precipitation in typical cities on the north slope of Tianshan Mountain in Xinjiang during 2010–2019. *Atmos* 13:646. <https://doi.org/10.3390/atmos13050646>
- Zhou X, Zhang TJ, Li ZQ, Tao Y, Wang FT, Zhang X et al (2018) Particulate and gaseous pollutants in a petrochemical industrialized valley city, Western China during 2013–2016. *Environ Sci Pollut Res* 25:15174–15190. <https://doi.org/10.1007/s11356-018-1670-6>
- Zhou W, Chen C, Lei L, Fu PQ, Sun YL (2020) Temporal variations and spatial distributions of gaseous and particulate air pollutants and their health risks during 2015–2019 in China. *Environ Pollut* 272:116031. <https://doi.org/10.1016/j.envpol.2020.116031>
- Zou XK, Zhai PM (2004) Relationship between vegetation coverage and spring dust storms over northern China. *J Geophys Res Atmos* 109:D03104. <https://doi.org/10.1029/2003jd003913>

Publisher's note Springer Nature remains neutral with regard to jurisdictional claims in published maps and institutional affiliations.

Springer Nature or its licensor (e.g. a society or other partner) holds exclusive rights to this article under a publishing agreement with the author(s) or other rightsholder(s); author self-archiving of the accepted manuscript version of this article is solely governed by the terms of such publishing agreement and applicable law.